POLITECNICO DI TORINO

College of Engineering and Management

Master of Science in Engineering and Management

Master of Science Thesis

Analysis of the customers' needs concerning the structural analysis of pole supporting signs/ lighting and development of a related calculation methodology

Supervisor:
Domenico Augusto Maisano

Candidate:
Aliakbar Babajani

June 2021

Abstract

Road safety is a market numerous companies are working on and trying to expand their role on. These days there are many road restrain systems implemented to increase safety in road transportation. Each equipment in this issue should have specific requirement to get certificate to being installed on roads. It is several decades that some companies are playing role to decrease cost of getting certificate for road restrain systems manufactures. Main cost in this field is car crash test and the manufactures pay money for structural analysis to know their product is compatible to the predefined regulations to save money and avoid spending money on crash test as much as possible.

In this thesis, at the beginning we discuss on the current situation of road restrain systems regulations, the influence of structural analysis in this scope, we make a brief explanation of the company in which this project has been implemented and the current standard is being followed in Europe.

Then in the second chapter, there are some definitions for basic equations have been used during our analyses and evaluations. To investigate scientifically the regulations in this topic there is not any other choice to go a little bit in depth of structural analysis basic and methods. This is what explained in second chapter and on this basis, the result reported on next chapter.

The most important part is chapter three that we tried to present a complete method covering all types of poles' geometries. In this chapter, you observe how the current standard performed in the evaluation of structures and the essential role a valid numerical simulation plays.

As you will see, at the end of this thesis, we could find a cheaper way of evaluation for poles with simple structures, and for complex geometries we should refer to numerical simulations. To get valid result in this latter one, a solution to cover common challenges in numerical simulation has been provided. At the end, there are two appendices to explain the analyses presented in chapter three in more detail.

Keywords: Road safety regulations, Structural analysis, sign and light poles, Numerical simulation

Table of Contents

List of tables:

List of figiures:

1 Introduction

1.1 Thesis Scope

Here, in twenty-one century one of the most important ways of transportation are cars and vehicles that all kinds of them need roads to move on. Always safety was an important parameter in transportation in which roads play an important role. Road safety is essential to the well-being of people and communities and vital for economic growth and prosperity. The potential for road infrastructure safety treatments to provide a certain and immediate reduction in crash likelihood and severity is well recognized. With adequate resources, infrastructure has the ability to eliminate nearly all fatal and serious crash outcomes. Many national and provincial road safety strategies have highlighted the role of infrastructure in making progress towards a Safe System.

Regarding this point, each country defines and applies specific standards to the road infrastructures and after passing these standards the manufacturer is allowed to install its product on roads. After making an obligation for manufacturers to follow the standard, it is imperative firstly to have a safe pole in front of car crashes. Secondly, the regulations should cover all types of poles and present a correct way to check the safety. Here, in this thesis, we want to investigate the standards considered for light and sign poles and evaluate how much the current standard is able to cover diverse geometries applied for poles.

1.2 The necessity of performing analysis on poles

Actually, GDTech is an engineering consultant company especially working on car crash simulation. After 2000, it is compulsory for road restrain system manufactures to pass car crash tests for any new product that they have the plan to produce. The cost of the test is so much so this is the time that simulation can play an important role to reduce costs. Customers are producers of Road Restraint Systems, Bridge Barriers, Poles [Lighting & Signs], Security Products, Circuits, and Industrial Protections. They ask GDTech to evaluate the strength of their new designs in front of common load factors defined in EN standards. In this way, when the result of the evaluation was satisfying the producer can test the product in a real test. Consequently, the manufacturer can save a considerable amount of money because the cost of the test is expensive and with getting advantage of car crash simulation, it is not necessary for them to pay for the test several times.

GDTech is mainly active in the calculation of passive safety poles, such as a signpost, adapted foundations via simulation of crash tests according to EN12767 or US standards. GDTech is one of the active representatives of Belgium in TC226 / WG10 (working group responsible for drafting EN12767).

1.3 Work environment of GDTech

GDTech is a Belgian engineering office of more than 200 employees specialized in calculation/ optimization/ simulation/crash test/certification of roadside safety equipment (safety barriers, …) to comply with European EN1317, American NCHRP350/MASH, Russian GOST or equivalent standards. They have a very high success rate of nearly 80% in calculation/ prediction in recent years which helped their customers to avoid risk and optimize their products. Simulations can be used during the design phase of a new product as well as for getting a direct certification of a modified version of a tested product (without the need to perform a new crash) or even adaptation to particular site conditions. Most of their customers are manufacturers of road safety equipment, resellers, or installation companies but they are open to any kind of firm.

GDTech has a team of multidisciplinary consultants being able to strengthen its customer's teams of designers, engineers, etc. This company can also make available its IT resources, thereby adapting to the specific needs of its customers.

Without being exhaustive, the sectors where GDTech employees can intervene on customer's site are:

Design drafter

Study engineer

Calculation engineer

Modeling engineer

Project manager

Documentation engineer

Exploitation engineer

Test technician

Methods agent

Materials engineer

Logistician

Quality engineer

1.4 What is EN12767 standard?

It's been estimated that vehicle collisions with rigid roadside features such as signposts and streetlights cause over 15% of all road fatalities. In the UK alone, there are around 100 deaths and 3,000 serious injuries every year, as a result of vehicles hitting street furniture. To tackle both the human cost and the impact on the European economy, the European standard EN 12767 was introduced in 2000, stipulating that all roadside furniture on roads with a speed limit over 50 km/h should be passively friendly (crash friendly). Since then, EN 12767 has been constantly reviewed with adjustments made every 5-10 years [1].

This document, EN12767, specifies performance test procedures to determine the passive safety properties of support structures (A passive safety feature is a system that does not do any work until it is called to action. These features become active during an accident and work to minimize damage and reduce the risk of injury during the time of impact. These devices automatically deploy when the car gets into a crash) such as lighting columns, sign posts, signal supports, structural elements, foundations, detachable products, and any other components used to support a particular item of equipment on the roadside.

This document provides a common basis for the vehicle impact testing of items of road equipment support structures.

More and more studies in the field of road safety improvement focus on the development of passive safety devices. The objective is to design devices capable of absorbing shocks to reduce impacts on vehicles.

2 Governing equation

In this thesis, we want to analyze some structural behavior of sign poles which needs some basic structural information about the metals behavior. In this chapter we review briefly these fundamental equations.

2.1 Stress in the members of a structure

- **Axial Stress**

  The force per unit area is called the stress and is denoted by the Greek letter σ (sigma). The stress in a member of cross-sectional area A subjected to an axial load P is obtained by dividing the magnitude P of the load by the area A:

$$\sigma = \frac{P}{A}$$

- **Shearing Stress**

  Dividing the shear P by the area A of the cross section, you obtain the average shearing stress in the section.

$$\tau_{ave} = \frac{P}{A}$$

- **Allowable Load and Allowable Stress: Factor of Safety**

  The maximum load that a structural member or a machine component will be allowed to carry under normal conditions is considerably smaller than the ultimate load. This smaller load is the allowable load (sometimes called the working or design load). Thus, only a fraction of the ultimate-load capacity of the member is used when the allowable load is applied. The remaining portion of the load-carrying capacity of the member is kept in reserve to assure its safe performance [2]. The ratio of the ultimate load to the allowable load is the factor of safety:

$$\text{Factor of safety} \;=\; \text{F.S.} = \frac{\text{ultimate load}}{\text{allowable load}}$$

An alternative definition of the factor of safety is based on the use of stresses:

$$\text{Factor of safety} \; = \; \text{F.S.} = \frac{\text{ultimate stress}}{\text{allowable stress}}$$

These two expressions are identical when a linear relationship exists between the load and the stress.

In some fields of engineering, the margin of safety is used in place of the factor of safety. The margin of safety is defined as the factor of safety minus one; that is, margin of safety = F.S. - 1.00.

- **Normal Strain Under Axial Loading**

We define the normal strain in a rod under axial loading as the deformation per unit length of that rod, or the change in length of the rod divided by its original length. The normal strain, ε (Greek letter epsilon), is

$$\varepsilon = \frac{\delta}{L}$$

Plotting the stress $\sigma = P/A$ against the strain $\varepsilon = \delta/L$ results in a curve that is characteristic of the properties of the material but does not depend upon the dimensions of the specimen used. This curve is called a stress-strain diagram [2].

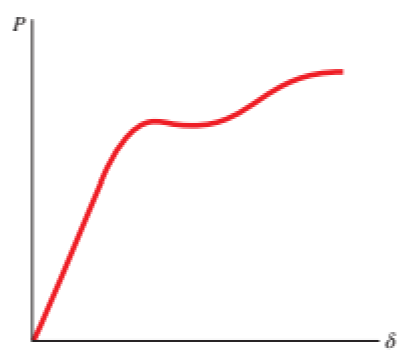

Figure 2-1 Load-Deformation diagram

- **Hooke's Law; Modulus of Elasticity**

Modulus of Elasticity. Most engineering structures are designed to undergo relatively small deformations, involving only the straight-line portion of the corresponding stress-strain diagram. For that initial portion of the diagram the stress σ is directly proportional to the strain ε:

$$\sigma = E\varepsilon$$

This is known as Hooke's law, after Robert Hooke (1635–1703). The coefficient E of the material is the modulus of elasticity or Young's modulus, after the English scientist Thomas Young (1773–1829). Since the strain ε is a dimensionless quantity, E is expressed in the same units as stress σ in pascals or one of its multiples for SI units and in psi or ksi for U.S. customary units [2].

- **Shearing Stress**

The shearing stress at any distance ρ from the axis of the shaft is the following Equation and are known as the elastic torsion formulas.

$$\tau = \frac{T\rho}{J}, \qquad \tau_{max} = \frac{Tc}{J}$$

Recall from statics that the polar moment of inertia of a circle of radius c is J = 1/2 πc^4. For a hollow circular shaft of inner radius c1 and outer radius c2, the polar moment of inertia is

$$J = \frac{1}{2}\pi c_2^4 - \frac{1}{2}\pi c_1^4 = \frac{1}{2}\pi(c_2^4 - c_1^4)$$

When SI metric units are used in, T is given in Nm, c or ρ in meters, and J in m^4. The resulting shearing stress is given in N/m^2, that is, pascals (Pa).

- **Symmetric Members in in Pure Bending (Internal Moment and Stress Relations)**

For pure bending the neutral axis passes through the centroid of the cross section and I is the moment of inertia or second moment of area of the cross section with respect to a central axis perpendicular to the plane of the couple M. we obtain the normal stress σ x at any distance y from the neutral axis:

$$\sigma_x = -\frac{My}{I}, \qquad \sigma_m = -\frac{Mc}{I}$$

The normal stress σ_x caused by the bending or "flexing" of the member is often referred to as the flexural stress. The stress is compressive ($\sigma_x < 0$) above the neutral axis ($y > 0$) when the bending moment M is positive and tensile ($\sigma_x > 0$) when M is negative.

- **Maximum-Distortion-Energy Criterion (von Mises criterion)**

The von Mises stress (σ_v) is used to predict yielding of materials under complex loading from the results of uniaxial tensile tests. Here, a given structural component is safe as long as the maximum value of the distortion energy per unit volume in that material remains smaller than the distortion energy per unit volume required to cause yield in a tensile-test specimen of the same material. Thus, we define

$$\sigma_v = \sqrt{\frac{(\sigma_1 - \sigma_2)^2 + (\sigma_2 - \sigma_3)^2 + (\sigma_3 - \sigma_1)^2}{2}}$$

where each σ is the stress in principal direction [2].

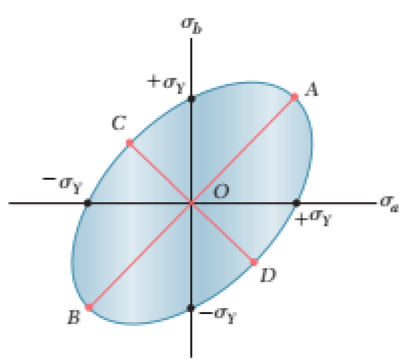

Figure 2-2 Von Mises surface based on maximum-distortion-energy criterion

2.2 Making simple some common calculations

To make it easier to find the solution during calculations we can mention the most common ones in the following tables:

- **Moments of Inertia**

Table 2-1 Moments of Inertia of Common Geometric Shapes

Rectangle	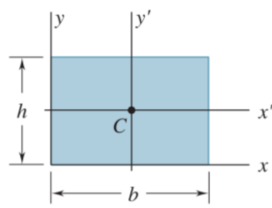	$\bar{I}_{x'} = \frac{1}{12}bh^3$ $\bar{I}_{y'} = \frac{1}{12}b^3h$ $I_x = \frac{1}{3}bh^3$ $I_y = \frac{1}{3}b^3h$ $J_C = \frac{1}{12}bh(b^2 + h^2)$
Circle	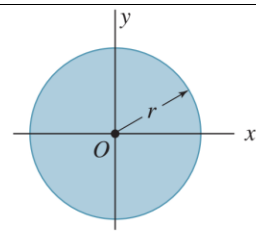	$\bar{I}_x = \bar{I}_y = \frac{1}{4}\pi r^4$ $J_O = \frac{1}{2}\pi r^4$

- **Deflections and Slopes**

Table 2-2 Beam Deflections and Slopes

Beam and Loading	Elastic Curve	Maximum Deflection	Slope at End	Equation of Elastic Curve
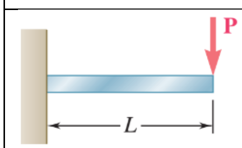	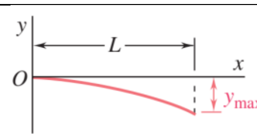	$-\dfrac{PL^3}{3EI}$	$-\dfrac{PL^2}{2EI}$	$y = -\dfrac{P}{6EI}(x^3 - 3Lx^2)$
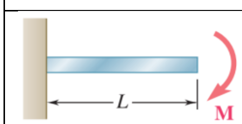	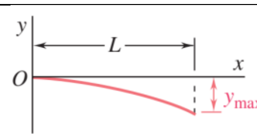	$-\dfrac{ML^2}{2EI}$	$-\dfrac{ML}{EI}$	$y = -\dfrac{M}{2EI}x^2$

3 A complete covering method for poles evaluation

One branch of GDTech customers are light and sign poles producers. Each pole may have a different cross-section, height, and material in which make it necessary to have exclusive calculation. In this study, the aim is to find an easy methodology to evaluate any kind of pole.

First, we want to find a simple way of evaluation for poles having simple cross-section, which make it possible to do the strength calculation with the analytical method and without the help of simulation. **Secondly**, make a simulation for a pole with complex geometry in ABAQUS software and find a method to answer the common challenges in this process. We want to find an answer to the challenges that occur in poles simulations and find a method to answer these problems not only for one case but also any pole with complex geometry.

3.1 Making an excel file to calculate any pole with simple geometry

In this step, we want to define a fast method to know whether the pole is safe or not. In other words, on the basis of EN standards, there are some specified loads and conditions that the pole should be checked to considered as a safe pole. Consequently, we want to make an excel file having these fixed loads and predefined conditions, and just by updating the file for each geometry and material of the new sign, we understand easily how much strength the sign has.

Already, in the previous version of the European standard for vertical traffic signs (EN 12899-1: 2001), the issue was "stability" to the existing or future Euro codes reference. In the new version, this approach is further refined and serves the mechanical performance of vertical traffic signs (both the overall construction and the parts) expressed as the deformation under the influence of a certain load (or loads of cumulative). For those loads and deformations, the standard provides a number of options [1]. By the following mathematical model can verify for a limited number of simple cases whether the stability requirements for the support are met or not. Note that the mechanical properties of the board are not taken into account here.

3.2 How the excel file works

3.2.1 General data

There are some input parameters related to the pole (General data). With filling pink cells as the input, other cells calculated automatically.

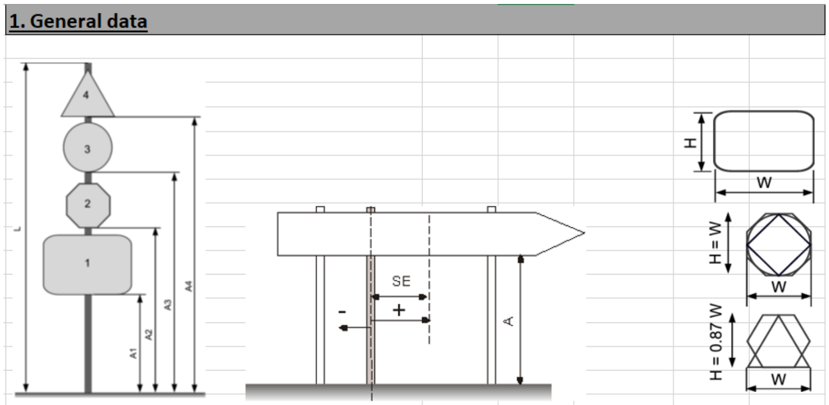

Figure 3-1 schematic picture of possible shapes for singns

1.Sign data including

- Sign number: it is possible to have even four sign installed on a pole
- Sign shape: Circular, Triangular, Diamond, Hexagonal, Octagonal, Rectangular
- Sign surface (Sign width, Sign Height)
- Height above ground
- Sign surface eccentricity SE
- Height of the CoG (Center of Gravity)

Signs data

Sign number (maximum 4)	Sign 1	Sign 2	Sign 3	Sign 4
Sign Shape	Circular	None	None	None
Sign Width W [m]	1			0
Sign Height H [m]	1			0
Height above ground A [m]	1			0
Sign surface eccentricity SE [m] [+ or -]	0.0285			0
Sign surface [m²]	0.785			0
Height of the CoG [m]	1.5	0	0	0

Circular
Diamond
Hexagonal
None
Octogonal
Rectangular
Triangular

Figure 3-2 the way input data imported in for the sign

The model is only applicable for constructions with one or two support posts. The point load according to the standard only occurs in one place. The simultaneous effect of torsion and simple bending is not taken into account. The height of the support posts (in relation to ground level) is less than 10 m. The self-weight of the structure is taken into account. For evenly distributed loads (wind load) on a surface, the calculation is each time based on the total resulting load that occurs in the center of the loaded surface.

2. Supports data including

Number of Supports

Material (we need to consider Yield of stress related to each material in our calculation)

Cross section (two type of cross section (SHS or CHS) is considered and the formulation will be updated to the user choice)

Outer Diameter, Dp [mm]

Wall Thickness, T [mm]

Total Length of Support, L [m]

Moment of Inertia, I [mm^4]

Modulus of Elasticity, E [N/mm^2]

Shear modulus, G [N/mm^2]

Support Stiffness, EI [kNm^2]

Torsional constant, IT [mm^4]

Resistance modulus, W [mm^3]

Shear area of the CS, Av [mm^2]

Torsion area of the CS, Am [mm^2]

Supports data

Number of Supports	1	
Material	Steel S	235
Cross section	CHS	
Outer Diameter, Dp [mm]	57	
Wall Thickness, T [mm]	5	
Total Length of Support, L [m]	2.00	
Moment of Inertia, I [mm^4]	2.79E+05	
Modulus of Elasticity, E [N/mm^2]	2.10E+05	
Shear modulus, G [N/mm^2]	8.10E+04	
Support Stiffness, EI [KNm^2]	58.51	
Torsional constant, I_T [mm^4]	5.57E+05	
Resistance modulus, W [mm3]	9776.7	
Shear area of the CS, Av [mm^2]	520.0	
Torsion area of the CS, Am [mm^2]	2123.7	

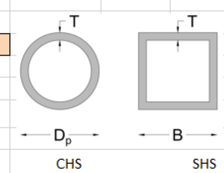

Figure 3-3 the way input data imported in for the support

3. Loading conditions

Wind load (per class) [kN/m^2]

Point load (per class) [kN]

Wind actions shall be calculated in accordance with EN 1991-1-4. The calculations shall identify whether they are based on a 25-year or a 50-year reference wind speed. The reference wind speed shall be appropriate to the sign location taken from the location data. The wind load shall be multiplied by the shape factor. The shape factor for flat signs is 1.20. The wind pressure shall be applied as a uniformly distributed load over the area of the sign plate and act at the center of pressure of the sign plate in order to calculate the bending moments in the supports and sign plate. The eccentricity value shall be declared in the requirements and in the evaluation report of the product. The deflections of sign plates are evaluated relative to the supports. The deflections of supports are evaluated separately [1].

4. Temporary deflection criteria

Maximum temporary deflection - Bending [mm/m]

Maximum temporary deflection - Torsion [°/m]

The wind load for calculating the temporary deflection shall be based on the wind loads multiplied by 0.56, and no partial action and material factors are applied. The factor of 0.56 is derived from the 50-year wind speed reduction to one-year wind speeds (EN 1991-1-4).

5. Permanent deflections

Permanent deflections shall be assessed using the following loads: 25 year or 50-year wind load, dynamic snow load, point load and dead load. The partial action and material factors are applied. When the structural performance is evaluated by means of a physical test, the maximum permanent deflection shall not exceed 20 % of the temporary deflection using the same load [1]. This takes into account the slack in the fixings and other non-elastic phenomena.

When the structural performance is evaluated by calculation, the material stresses shall not exceed the elastic limit.

Normal stresses - Bending, σ [N/mm²]	156.17				< 235
Check: Bending resistance	70%				PASS
Wind Load: Torsion					
	Sign 1	Sign 2	Sign 3	Sign 4	
Design Wind Load [kN]	1.018	0	0	0	
Torsion at the level of each sign [kNm]	0.029009	0	0	0	
Total Torsion at the base of the suport [kNm]	0.029009467				
Shear yield limit stress, τ_y [N/mm2]	135.7				
Torsion capacity, T_{Rd} [kNm]	2.53				
Shear stresses - Torsion, τ_t [N/mm²]	1.37				< 135.7
Check: Torsion resistance	1%				PASS
Wind Load: Shear					
	Sign 1	Sign 2	Sign 3	Sign 4	
Design Wind Load [kN]	1.018	0	0	0	
Design Shear Force, V_{Ed} [kN]	1.018				
Shear Capacity of the suport, V_{Rd} [kN]	70.56				
Shear stresses - Shear, τ [N/mm²]	1.96				< 135.7
Check: Shear resistance	2%				PASS
Wind Load: Overall check					
Equivalent (von Mises) stresses - Bending, σ_e [N/mm²]	156.3				
Elastic stress verification	0.40		<= 1		PASS

Figure 3-4 how we can see the design is safe or not

In this excel file, when the safety factor is greater than one or the stress is lower than the Yield stress, the excel display it in green color and print 'PASS' otherwise it would be in red color and print 'FAIL'.

As it was mentioned before, this file defined to calculate the stress and simply understand whether the structure is safe or not (for poles with continuous Regular polygons cross-sections). You can find more details of this Excel file in Appendix 1 and how the data imported and the result displayed.

3.3 Validation the excel file with Numerical simulation

3.3.1 Material

The actual design prescriptions given by EN 12899-1:2007 are assuming that the material will present an elastic behavior under the specific loads corresponding to 25 or 50 years return period. The deformation of the supporting structure under the action of these loading scenarios shall stay in the elastic region, see EN 12899-1:2007 (5.4.3). Therefore, there assumed that the material will behave in a perfectly elastic way, but the maximum stress on the cross-section of the members shall not exceed the yield limit, in such a way the deformations will remain in the elastic range.

Assumption: Steel - perfectly **linear elastic** behavior

Table 3-1 Mechanical properties for the support

Parameter Value	Value
Young's modulus, E [MPa]	210000
Poisson's ratio, ν	0.3
Density, ρ [kg/m3]	7850

3.3.2 Model validation

It is intended to confront the actual design procedure for traffic sign-support poles according to the EN 12899-1:2007 standard and the results of a numerical simulation. In order to calibrate the numerical model and identify the potential sources of differences in the results, the simplest case of a supporting pole was analyzed using the two approaches.

3.3.3 Case study: Signal post (full strength CHS cross section post)

An assembly comprising a vertical base fixed CHS section pole and a baseplate fixed through 4 anchors to a concrete foundation block will be analyzed hereafter. The main goal is to confirm that the actual design procedure based on classical analytical relations and the numerical simulations are providing very close results, confirming that the use of numerical simulations for more complex cases is an appropriate and reliable approach.

The CHS pole will be used as a support for a circular traffic sign; the main long-term loads acting on such a structure corresponds to the wind action.

- Pole cross-section: CHS 57x5

- Pole length: 2 m

- Base plate: 25 mm thick, considered rigid and fully fixed at the interface between the concrete foundation and the plate.

- Circular sign diameter: 1 m => Area=0.785 m^2

3.3.3.1 Numerical model

The assembly comprising the vertical pole and the base plate was modeled in Abaqus (DS SIMULIA SUITE 2020 version) using shell type elements.

Abaqus as a part of SIMULIA family of codes is a multiphysics modeling and simulation software. Abaqus Standard is used for problems solved by implicit schemes and Abaqus Explicit for high-speed dynamic problems. As one of the major commercial FE software programs, Abaqus is compatible with a lot of other in-house or commercially available FE codes [3].

Here in this problem, the material was defined, as having a perfectly elastic behavior, the main goal for this analysis is to identify if the yield limit strength of the material is exceeded in any points of the cross-section when subjected to the permanent/long-term wind or point concentrated loads [4].

To have enough reliability of the results, in two ways the problem was simulated:

Firstly, only support without any part of base plate:

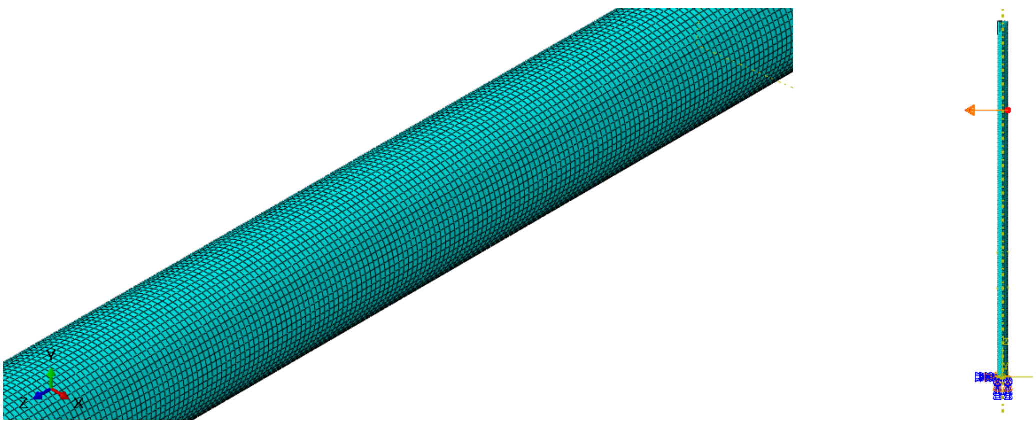

Figure 3-5 Model with only support and mesh 3D view plus boundary conditions

*Note: The bottom of the support is assumed to be rigid and fully fixed at the all-around the bottom edge.

Secondly, the model that has support plus base plate:

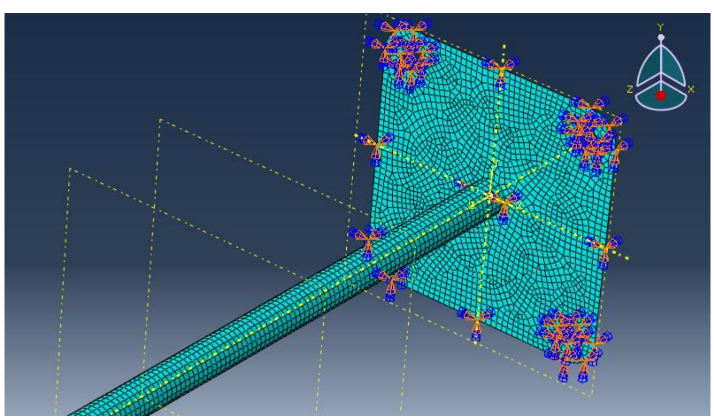

Figure 3-6 Second model and mesh 3D view plus boundary conditions

3.3.3.2 Loads

The main loads acting on such a structure were assessed considering the recommendations and prescriptions given in EN 12899-1:2007, making some general assumptions about the geographic position of the pole and the loading conditions.

Wind class: WL3 – wind pressure: 0.80 kN/m^2

Point load class: PL2 – concentrated load:

Temporary deflection criteria: - Bending: TDB3

- Torsion: TDT4

Considering the total area of the traffic sign panel (0.785 m^2) and the characteristic value for the wind pressure (0.80 kN/m^2), a concentrated load of 1.0 kN was applied at the top of the pole, replacing the wind pressure distributed on the traffic sign panel. A shape coefficient of 1.2 was considered when the design value of the wind pressure was computed (A < 2 m^2) and a partial safety factor of 1.35 was considered for the long-term value of the load.

$$F = 0.785 \times 0.8 \times 1.2 \times 1.35 = 1.01736\ kN$$

3.3.3.3 Results

For the analytical design approach an Excel spreadsheet, that follows the prescriptions of EN 12899-1:2007 and EN 1993-1-1:2005 was developed. It is intended to confront the results obtained using this approach to the ones provided by the numerical simulation. The main output parameters that will be checked are the distribution and the maximum value of the stresses on the cross-section at the base level of the pole and the maximum horizontal displacement at the upper free end of the pole.

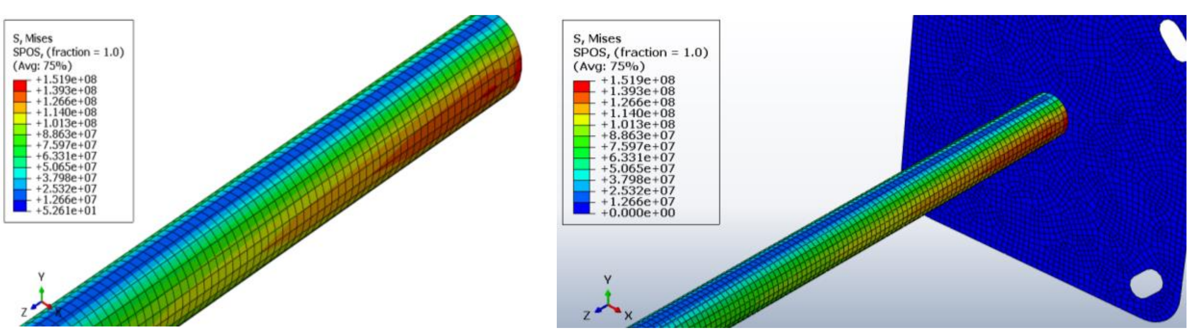

Figure 3-7 von Mises stress distribution [N/m^2]

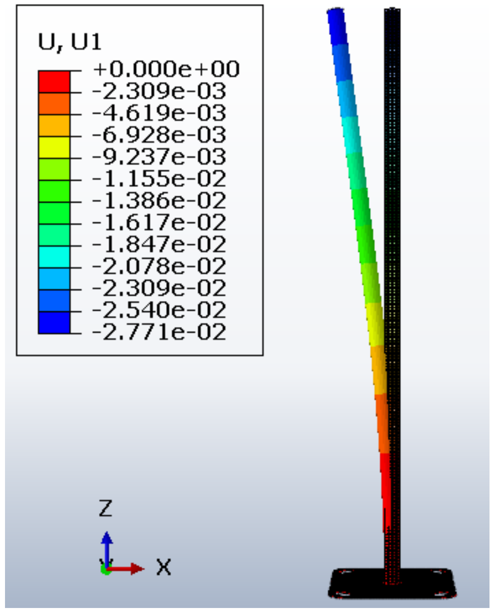

Figure 3-8 Horizontal deflection [m]

To have reliable numerical results, one grid study has performed for the model. Grid-independent means calculated results change so little along with a denser or looser grid that the truncation error can be ignored in numerical simulation. If the results tend towards identical, the grid can be considered as grid-independent [5]. The S22 results at a line of nodes (from the root towards the top of the support) have compared for seven different element sizes (0.003, 0.005, 0.006, 0.007, 0.008, 0.009, and 0.010)

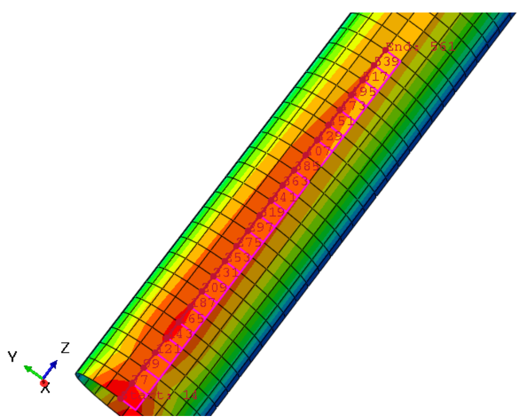

Figure 3-9 The selected path of nodes to report S22

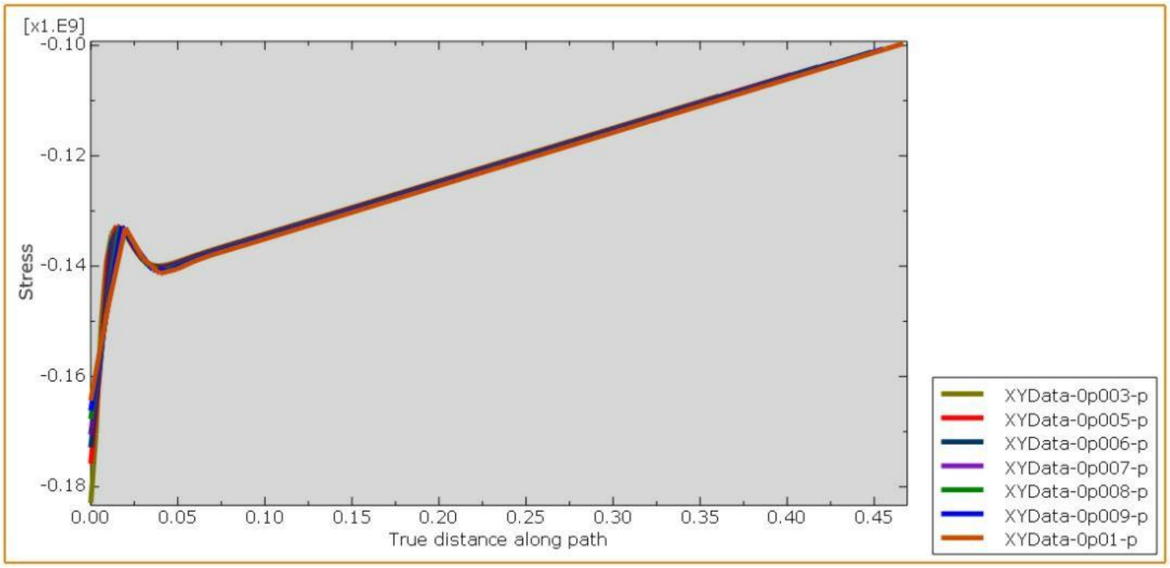

Figure 3-10 The amount of S22 at the path for different element sizes

First of all the comparison among these element sizes presents the same results at most all parts except the root point where the boundary conditions have been defined. Therefore, it is obvious that we have the influence of concentrate stress at the root, resulting in different stress for any different element size [6]. As the element size is smaller, the amount of stress reaches a larger amount. It is not related to physical reality and only stems from numerical simulation and its' way of solving the problem. Consequently, first, it should be considered some parts of error for stress amount in this region and in numerical simulation to report stress at the root, it is necessary to refer to some nodes at the neighbor of the root where there is the same result for different element sizes. In addition, returning to the analytical solution can lead to the correct stress amount and specify the amount of error in numerical simulation.

Secondly, the grid study, in the same way, has performed for the second model (the model which also includes the base inside) and the results are shown in the bellow picture:

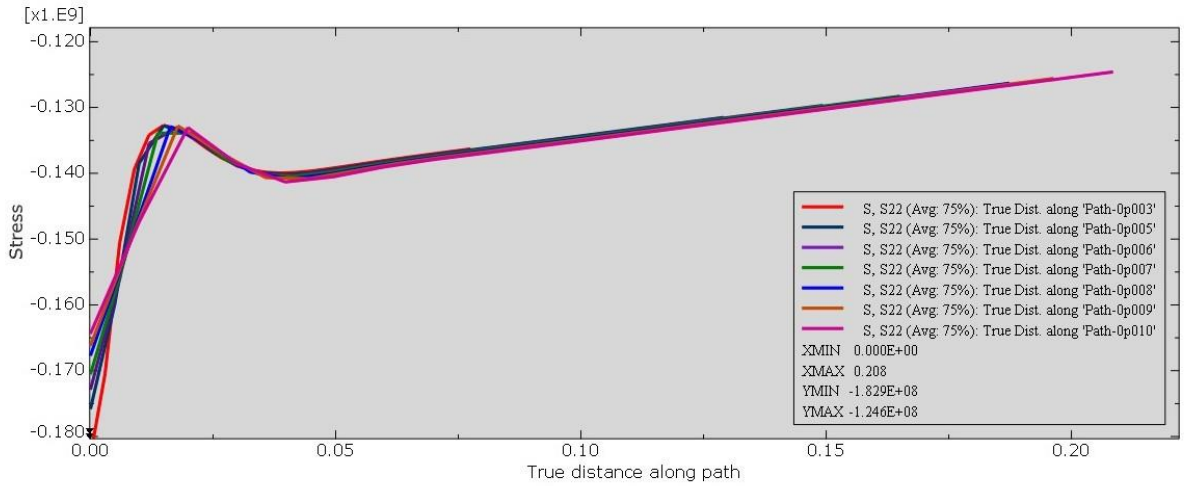

Figure 3-11 The amount of S22 at a path from root toward top of the support

In Figure 3-10 and Figure 3-11 , consider this point that with different element sizes, the position of nodes would be a little bit different in each size of the mesh. This gives cause for the difference to each stress curve in the above plots. Consequently, the comparison results in similar amounts of stress in these two models and for the other shapes of signs (when only the result of support is important) lead to the same results, it has less cost of computation to use only support model without base plate.

Table 3-2. Analysis output summary

Full strength section CHS 57x5	**Analytical approach EN 12899-1:2007**	**Numerical simulation Shell elements***	**Difference analytical/numerical**
S22 [N/mm^2]	156.17	155	0.75%
Top deflection [mm]	29.35	28.07	4.36%

*It is worth mentioning that the amount of stress at the external section points has reported because the region with more distance from the center of support has more stress and when using shell elements it should be considered.

3.3.4 Commentaries

- It is noticeable that for this particular case, the results obtained through the different approaches are very similar (less than 5% difference), thus it would be more logical to use the numerical model only for more complex applications that are not easy to be analyzed by means of analytical methods.

- Because the vertical member is mainly subjected to bending without axial compression force, the buckling check should consist of verification of possible loss of local stability of the member. However, the tubular cross-sections are usually classified as being class 1 and 2 of cross-sections. In this case, according to EN 1993-1-1:2005, the local buckling of the member occurs only after reaching the plastic potential of the member, after the plastic hinge development. Because the member is supposed to remain in the elastic range, as stated in the first section of this report, it can be assumed that for the class 1 and 2 of cross-sections, an explicit check of local buckling risk is not required.

- As EN 1993-1-1:2005 6.3.2.1 (2) states, the CHS and SHS sections are not susceptible to lateral-torsional buckling, hence a check for lateral-torsional buckling is not required in this particular case.

- In addition to these two models, another way of modeling was tested. The model has included the base plate and the support in two different shell models having tied at their contact edge. The result was similar and without any specific difference.

3.3.5 Case study: Signal post (Full strength SHS cross section post)

3.3.5.1 General data

It is intended to assess the differences between the stress distributions at the base level of the pole using two different approaches, the one prescribed by the EN 12899-1:2007 standard and a numerical simulation.

- Section: SHS 250x5.9

- Wind class: WL3

- Point load class: PL2

- Temporary deflection criteria: - Bending: TDB3

- Torsion: TDT4

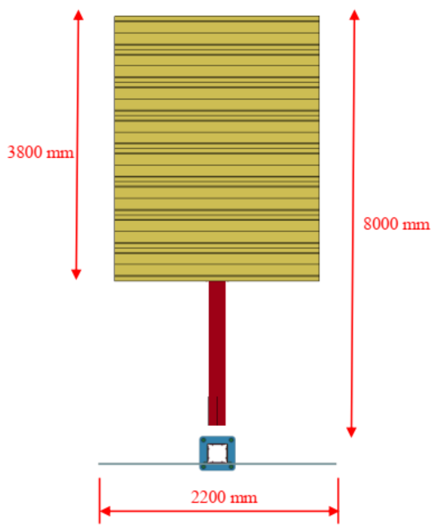

Figure 3-12 Real assembly

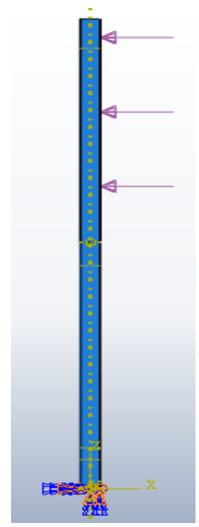

Figure 3-13 Simplified model

3.3.5.2 Numerical model

The numerical model has been developed in Abaqus (DS SIMULIA SUITE 2020 version). According to what observed for the circular cross-section model, this time only support with rectangular cross-section and without base plate implemented for the numerical model to simulate the real physical behavior. The bottom edge of support considered rigid and fully fixed. (Even if this latter point will lead to slightly different results when compared to the real ones, as the deformation capacity of the base plate and the redistribution of stresses due to this fact are neglected). The traffic sign panel was not modeled, but the wind pressure acting on it was considered according to its dimensions and load distribution way (one-way to the pole).

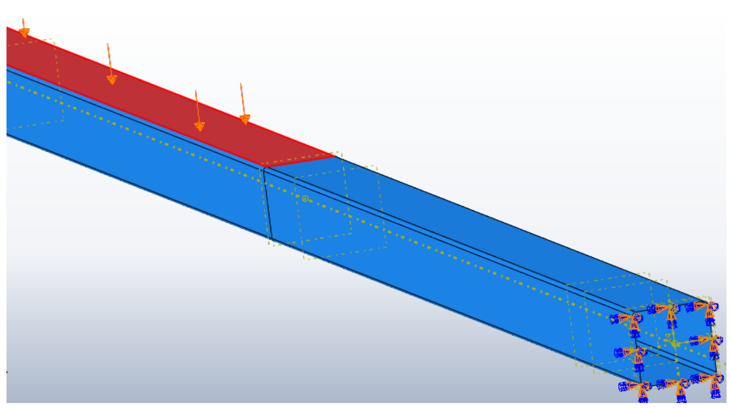

Figure 3-14 First model with only support and its' boundary conditions

3.3.5.3 Loading scenario

The loads associated to the wind action were assigned as pressure over one face of the SHS profile (see Figure 3-14), considering the tributary area of the sign panel. The model has been developed assuming a wind load class WL3, as prescribed by the EN 12899-1:2007 standard class, which implies the use of a characteristic wind pressure value of 0.80 kN/m^2. The design value of the wind pressure was computed considering a shape factor of 1.5 (A > 2 m^2) and a partial safety factor γ_F=1.35 (according to EN 12899-1:2007), thus obtaining a value of 1.62 kN/m^2.

$$A_{Sign\ cross\ section} = 3.8 \times 2.2 = 8.36\ m^2$$

$$F = 8.360 \times 0.8 \times 1.5 \times 1.35 = 13.54\ kN$$

Considering the tributary area of the sign panel and the surface of a SHS profile face, the magnitude of the surface pressure applied on the face of the SHS profile is 15.766 kN/m^2.

$$A_{Support\ cross\ section} = 3.8 \times 0.226 = 0.8588\ m^2$$

$$P = \frac{13.54 \times 10^3}{0.8588} = 15.766\ kpa$$

The loads corresponding to the temporary loading scenario are neglected, considering that the magnitude of these loads is less than the one of the permanent/long-term loads.

3.3.5.4 Results - Wind load

To have reliable numerical results, one grid study has performed for the model. The S22 results at a line of nodes (from the root towards the top of the support) have compared for seven different element sizes (0.003, 0.004, 0.005, 0.006, 0.007, 0.008, 0.009, and 0.010)

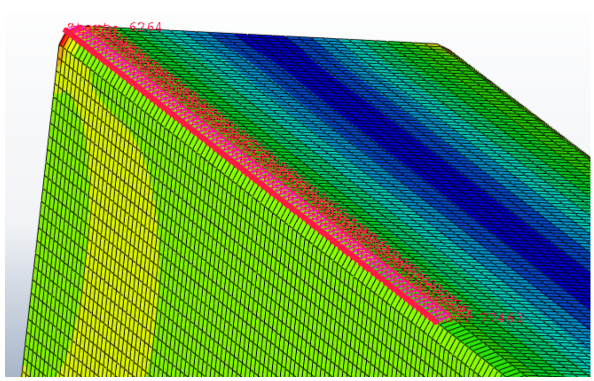

Figure 3-15 The selected path of nodes to report S22

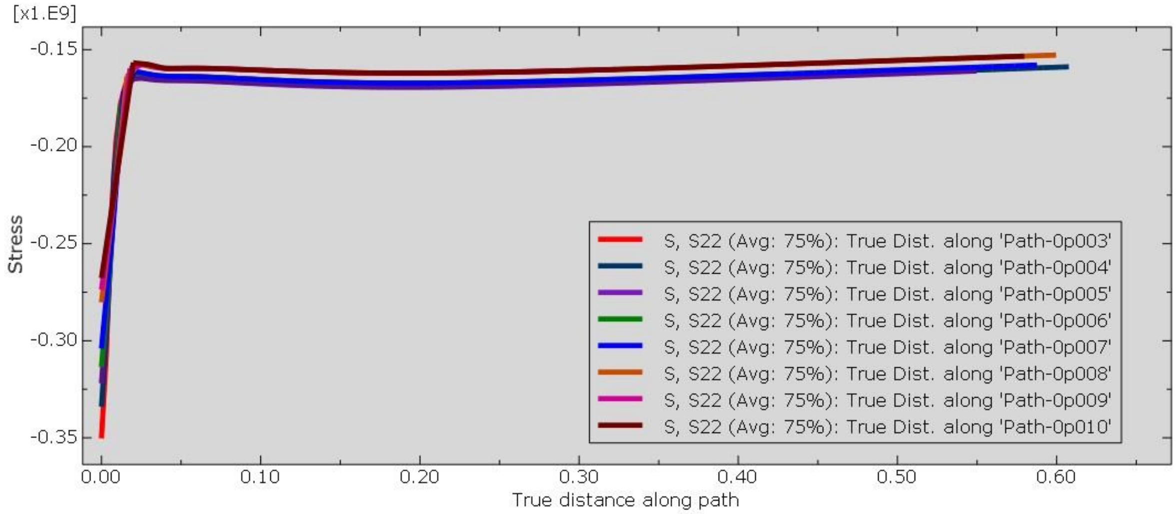

Figure 3-16 The amount of S22 at the path for different element sizes

Here, we have the same as what observed for the circular cross-section, there is the influence of concentrate stress at the bottom of the pole. To have the stress at the root it is necessary to go a little bit away from the root to have the correct stress amount. In addition, the cross-section is less simple, which is why the convergence is not as accurate as before.

In order to be able to compare the results of the two analysis methods, the average stress was computed along the tensioned face of the SHS profile (see the path (red line) in Figure 3-17). The von Mises yield criterion was considered for this particular operation, and the equivalent stresses obtained through the two approaches should be compared.

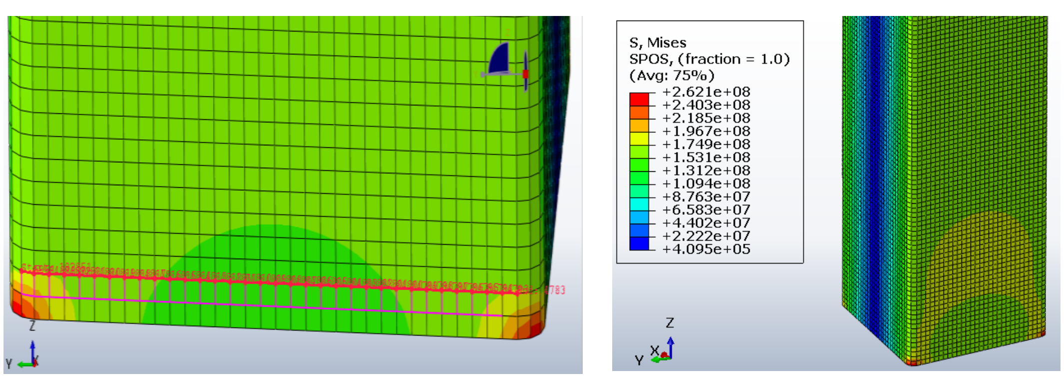

Figure 3-17 von Mises stress distribution and the red line path selected stress in root [N/m2]

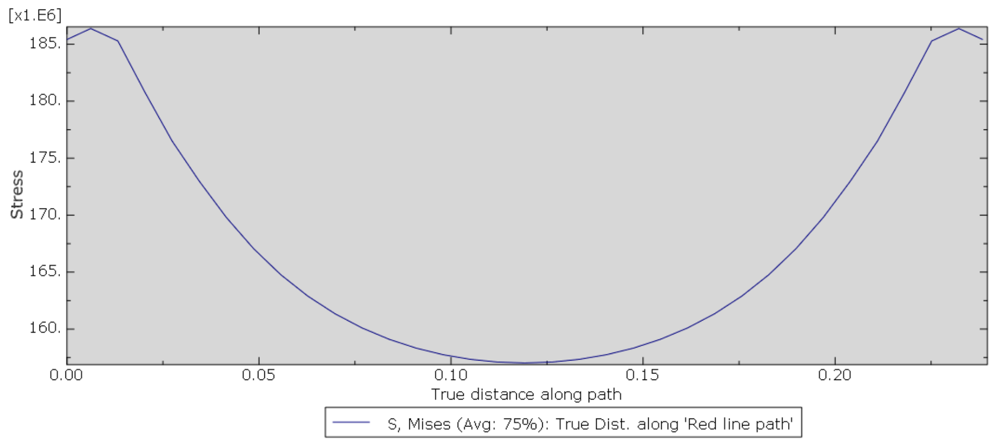

Figure 3-18 von Mises stress along the path on the tension side (red line - Figure 3-17) of the profile [N/m2]

Table 3-3 von Mises stress distribution along the path on the tension side of the SHS profile

Location on SHS edge [m]	Von Mises stress [MPa]	Average stress [Mpa]
0	185.41	
6.2135	186.38	
13.2775	185.29	
20.3407	180.77	
27.4038	176.50	
34.4667	172.98	
41.5297	169.79	
48.5926	167.06	
55.6555	164.78	
62.7183	162.89	
69.7812	161.35	
76.844	160.10	
83.9068	159.10	
90.9696	158.33	
98.0324	157.75	
105.095	157.34	
112.158	157.11	
119.221	157.03	168.08
126.283	157.11	
133.346	157.34	
140.409	157.75	
147.472	158.33	
154.535	159.10	
161.597	160.10	
168.66	161.35	
175.723	162.89	
182.786	164.78	
189.849	167.06	
196.912	169.79	
203.975	172.98	
211.038	176.50	
218.101	180.77	
225.164	185.29	
232.228	186.38	
238.441	185.41	

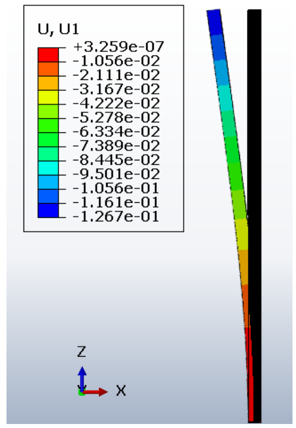

Figure 3-19 Horizontal deflection [m]

Full strength section SHS 250x5.9 Analytical approach EN 12899-1:2007 Numerical simulation Difference analytical/numerical Solid elements

Table 3-4 Analysis output summary

Full strength section SHS 250x5.9	**Analytical approach EN 12899-1:2007**	**Numerical simulation Shell elements***	**Difference analytical/numerical**
S22 [N/mm^2]	180.4	168.08	6.83%
Top deflection [mm]	125.07	126.7	1.28%

*It is worth mentioning that the amount of stress at the external section points has reported this is because the region with more distance from the center of support has more stress and when using shell elements it should be considered.

3.3.6 Commentaries:

- It is noticeable that in the case of SHS cross-section, even if the values for the horizontal displacements are very close and the difference between the two analysis methods is negligible, the values of the average equivalent stress are slightly different. These differences can be explained by the fact that, in this particular case, the shape of the cross-section is influencing the stress distribution – the corners of it acting as some stress concentrators.

3.4 Simulation one complex pole in ABAQUS

In the previous Excel file, we supposed that the cross-section of the pole is a fixed circle or rectangle; however, it is not what happened in all designs of poles. The cross-section may change from the bottom to the top; the pole is not a single part and made of connecting subparts with different and complex geometries. In these problems, numerical simulations with commercial software would be the way to check the structure strength [7]. There are some common challenges in these kinds of simulations that we want to find and define a method to these challenges. This is why in this step, first a complex pole is simulated with the Abaqus software to observe the challenges in a real problem and try to find a logical way to handle them [8].

3.4.1 Geometry (Part module)

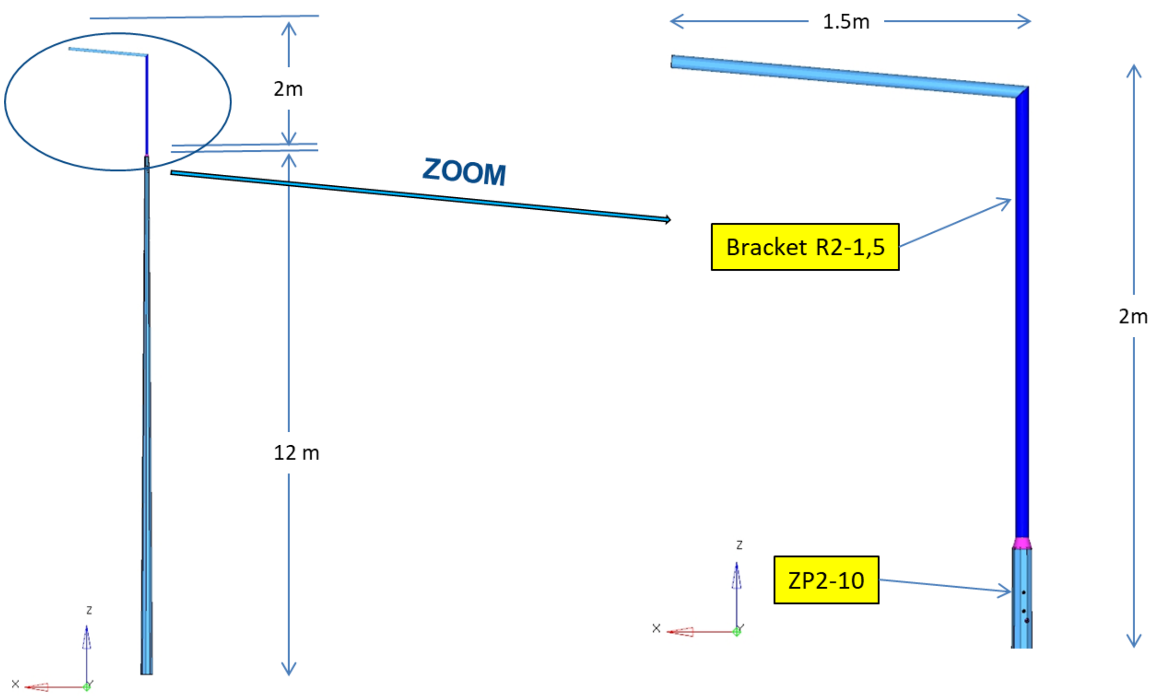

Figure 3-20 ZP2-10 & Bracket R2-1,5

As you see in Figure 3-20, this is the ZIP pole and we want to operate a static analysis to evaluate its strength. This complex pole is mainly made of three parts: ZP2-10 (upper and lower part), Bracket R2-1,5.

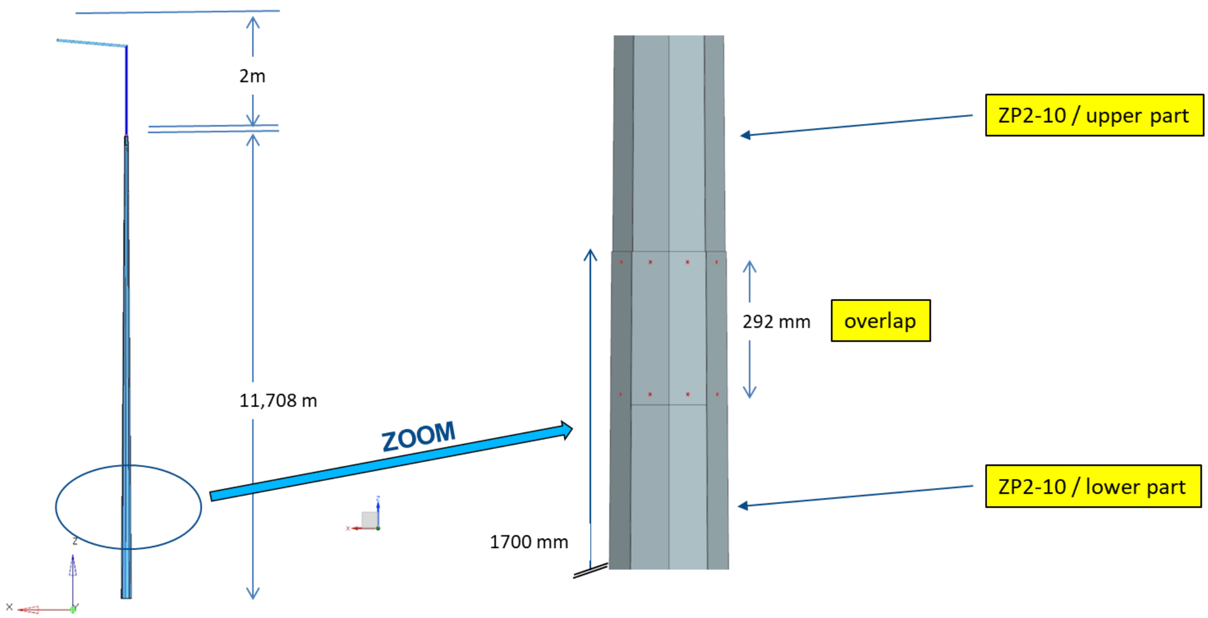

Figure 3-21 ZP2-10 & Bracket R2-1,5 – overlap

The first step is making a precise model of the pole in the Software. To do that, a 'stp' file of the model was imported in Abaqus and it was created without any error or failure. The main parts are all deformable, 3D and solid type.

3.4.2 Property module

The next step is defining the material properties (creating section) for each part and assigning this section for parts. The pole is made of steel and its detailed properties mentioned in the bellow table.

Table 3-5 Mechanical properties considered for the pole

Parameter Value	**Value**
Young's modulus [MPa]	210000
Poisson's ratio	0.3
Density [kg/m³]	7800
Yield strength [MPa]	340 – 420
Ultimate tensile strength [MPa]	410 – 510

Hypothesis: Mechanical behavior is perfectly linear elastic.

Other settings which implemented in Abaqus software are mentioned with the details in Appendix 2 to know exactly how the loads, boundary conditions, and other features are defined.

3.4.3 Visualization module

After running the job, the result would be ready in the Visualization module. First, we can observe the deflection. In Figure 3-22, total and deflections in the X direction are on the left side, and deflection in Z, Y directions are on the right side. The wind load implemented in the X direction, this is why the deflection in the Y and Z direction is considerably less than the X direction.

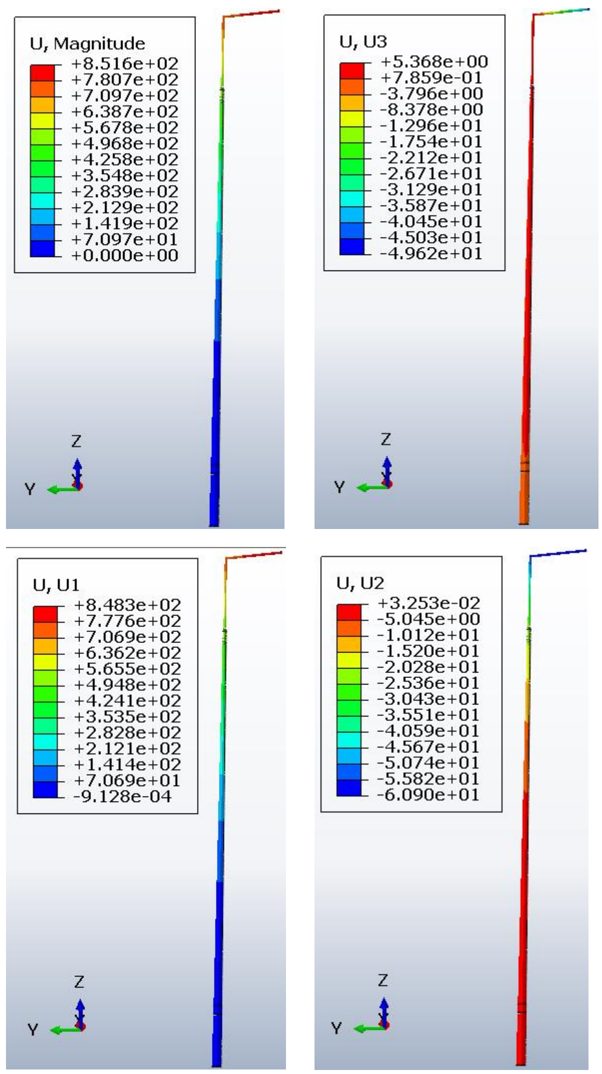

Figure 3-22 Deflection in different direction

After deflection, another important parameter to check the result is stress. In the next figures, we can see the amount of stress in each part.

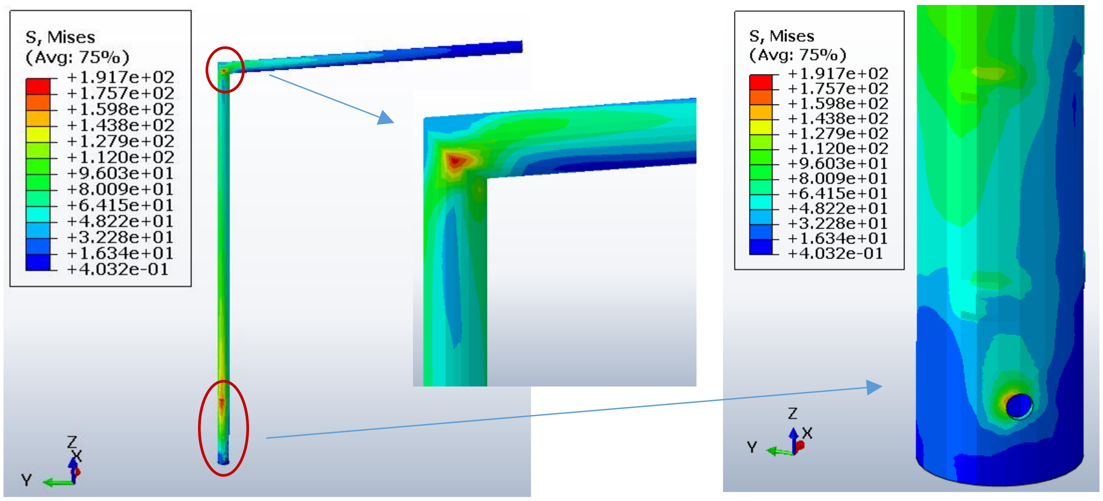

Figure 3-23 Von Mises stress contour in Bracket part

As you see, the maximum stress is in the regions bolts have contact with the Bracket. First, where bolts (M6) are in contact with ZP2 and Bracket to maintain Bracket, and secondly, where we have M10 to connect Bracket and ZP2 upper part.

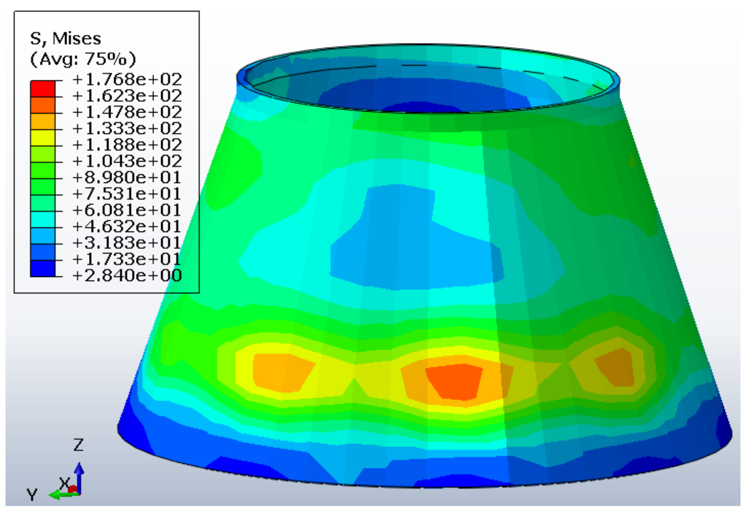

Figure 3-24 Von misses stress contour in Hat

For Hat, as it is clear in Figure 3-24, there is high stress in the regions that is in contact with ZP2. The cross-section of ZP2 is polygon resulting in discrete high-stress region.

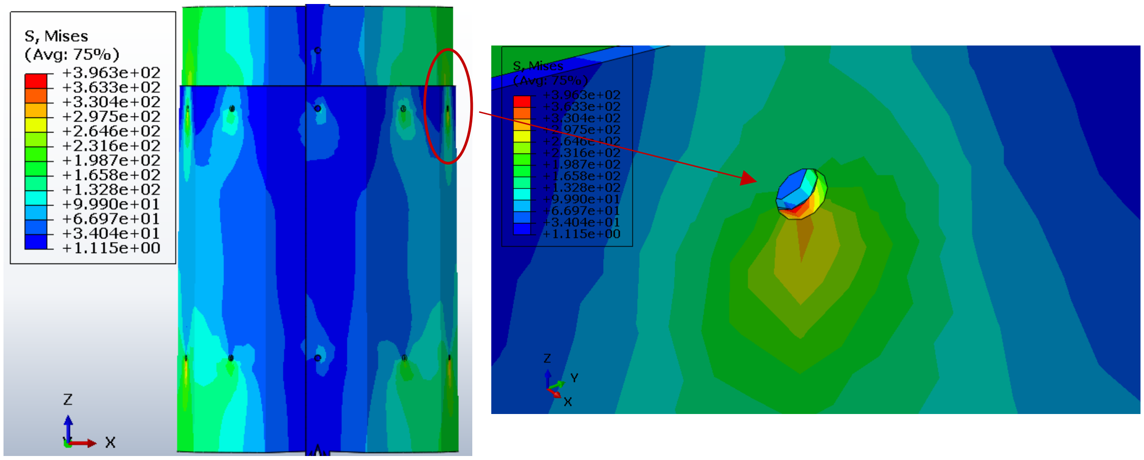

Figure 3-25 Stress results in the overlap region between upper and lower part of ZP2

In Figure 3-25, there is a display of overlap region of ZP2 upper part and lower part. As mentioned in the interaction module, there is a tied contact between the rivet and its contact region with ZP2. It is obvious that maximum stress in the overlap region and around rivets.

3.4.4 Calculation of safety factor 1

Now, it is the time to calculate safety factor (FS) for each part of the Pole. FS is the ratio between the yield stress of the pole material and the maximum stress we found in our result.

$$FS = \frac{YS}{\sigma_{VM}}$$

Consequently, the amount of FS for each part would be in the following table:

Table 3-6 FS values in the pole components

Part	Max σ_{VM} [MPa]	YS [MPa]	FS	MS
Pole ZP2-10 (upper)	297.5	420	1.4	0.4
Pole ZP2-10 (lower)	396.3	420	1.05	0.05
Hat	176.8	420	2.37	
Bracket	191.7	420	2.19	

If you pay attention, to calculate we just referred to the maximum stress that Abaqus reported for each part. Now, in this pole as an example of complex geometry, FS is always more than 1.0 but it is not far from 1.0 for ZP2 and Bracket. In the real world, most common structures have some margin of safety (predefined higher numbers than one such as two or more for FS) that should be considered to pass the structure and get the certificate. In other words, not only FS should be more than one, to have enough certainty of the structure strength it is common to define these numbers with enough distance than one in each industry [9]. In our structure, if we were sure that we do not have enough safety margin, for example with increasing the thickness or adding more rivets the stress decrease and can pass the defined margin of safety. Here, the problem is that in each part maximum stress is not in a region but only we have this maximum stress in one element or only one node of an element [8]. This phenomenon happened in all parts of the pole. We are using numerical simulation to solve the problem and when stress increases dramatically only in one element or node there is so much possibility of stress concentration. Therefore, we should investigate how much is the influence of stress concentration and after that again calculate FS. In this way, perhaps it is not necessary to increase the thickness or number of rivets which inevitably would increase the cost dramatically.

3.5 Finding a reliable method to report simulation result and overcome to the FEM limitations

Here, there is a serious problem with stress concentration when dealing with FEM software in complex geometry and we want to find a solution in dealing with stress singularities and concentrations.

In recent decades, the application of FEM (Finite Element Method) analysis developed and found its role as a popular inexpensive way of analysis [10]. Nevertheless currently, a higher number of engineers are struggling with simulations; in particular, they are trying to solve the stress singularities and concentrations in their problems [11]. These two problems are fundamental to understand the quality and validity of the simulation and it seems necessary in obtaining some design guidelines to tackle them.

3.5.1 Introduction

FEM analysis, as you may know already, allows finding stress and displacement inside a continuum domain. To perform a FEM analysis the domain must be divided into smaller and elementary elements. This procedure, known as discretization, is fundamental to obtain accurate results: as the dimension of the elementary elements becomes smaller generally the solution converges towards the exact problem solution [10].

This is not always true and this thesis illustrates some problems often users may encounter.

3.5.2 Applying and Interpreting Saint-Venant's Principle

All structural engineers use Saint-Venant's principle, whether actively or subconsciously. You can find various formulations of this principle in most structural mechanics textbooks, but its exact meaning is not obvious. Saint-Venant's principle tells us that the exact distribution of a load is not important far away from the loaded region, as long as the resultants of the load are correct. In this section, we will explore Saint-Venant's principle, particularly in the context of finite element (FE) analysis [12].

3.5.2.1 Simple Example: Analyzing Stresses at a Distance

We start with something quite simple: a thin rectangular plate with a circular hole at some distance from the loaded edge, which is being pulled axially. If we are interested in the stress concentration at the hole, then how important is the actual load distribution?

Three different load types are applied at the rightmost boundary:

1. A constant axial stress of 100 MPa

2. A symmetric parabolic stress distribution with peak amplitude 150 MPa

3. A centered point load with the same resultant as the two previous load cases

As seen in the plots below, the stress distribution at the hole is not affected by how the load is applied. The key here is, of course, that the hole is far enough from the load.

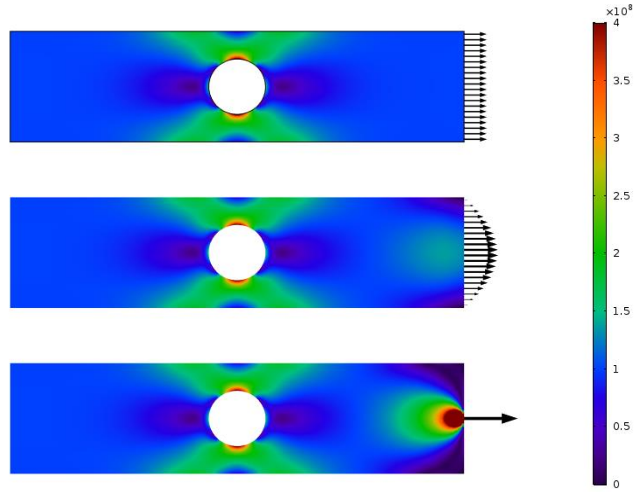

Figure 3-26 Von Mises stress contours for the three load cases.

By graphing the stress along a line, we can see that all three cases converge to each other at a distance from the edge, which is approximately equal to the width of the plate.

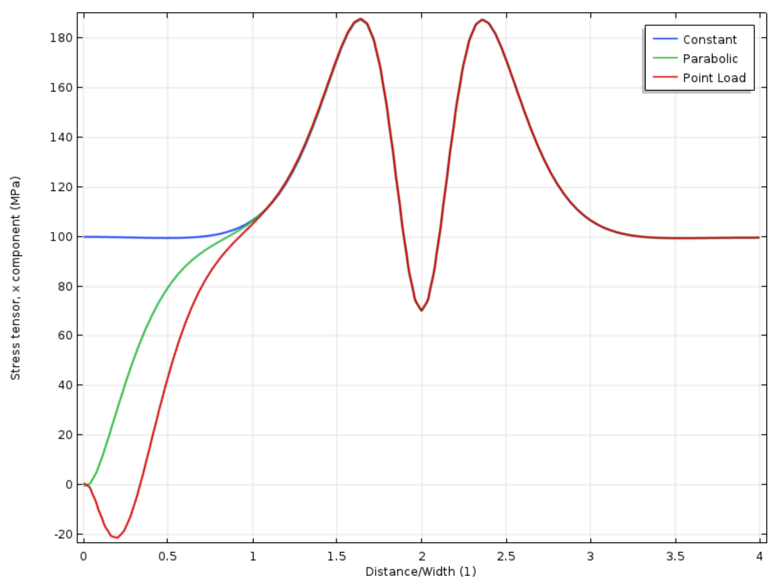

Figure 3-27 Stress along the upper edge as a function of the distance from the loaded boundary. The distance is normalized by the width of the plate.

If the hole is moved closer to the loaded boundary, we get another situation. The stress state around the hole now depends on the load distribution. However, even more interesting is that the distance to where the three stress fields agree now is twice as far from the loaded boundary. The application of Saint-Venant's principle requires that the stresses are free to redistribute. In this case, redistribution is partially blocked by the hole.

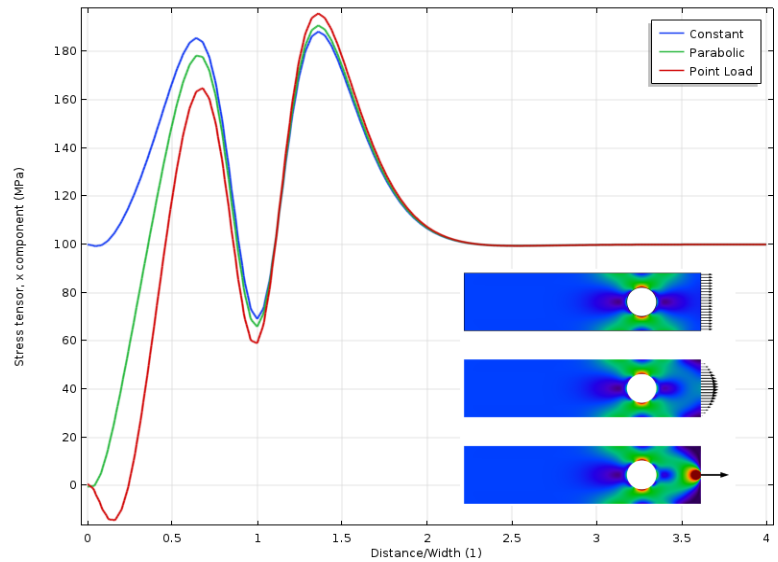

Figure 3-28 Stress along the upper edge with the hole closer to the loaded boundary.

Note that Saint-Venant's principle tells us there is no difference in the stress state at a distance that is in the linear dimension order of the loaded area. The loaded area to be taken into consideration, however, may not be the area that is actually loaded! This statement may sound strange, but think of it this way: When the hole is far away, we may compute the stress concentration factor using a handbook (mine says 3.5.7) rather than by an FE solution. The handbook approach contains an implicit assumption that the load is evenly distributed as in the first load case. So even if the actual load was applied to only a small part of the boundary, the critical distance in that case is related to the size of the whole boundary.

When solving the problem using the finite element method (FEM), then the hole can be arbitrarily close to the load. What sets the limit is that from the physical point of view, the load distribution is well defined. As soon as we make assumptions about redistribution, however, there is an implicit assumption about the load distribution, which may differ from the actual one [13].

3.5.3 Stress singularities

A stress singularity is defined as a point where the stress does not converge towards a specific value when the basic elements dimension is reduced. In these points, the stress level measured with a FEM analysis keeps increasing while the mesh is refined up to an infinite value [14].

Geometry highly affect the presence of these type of occurrences: **appliance of a point load, sharp re-entrant corners, corners of bodies in contact and point restraints** are the most common situations which should be avoided. These stress singularities does not affect the quality of the simulation: according to the St. Veneant's Principle (it explained in 0) it is possible to define a distance away from the singularity where stress results are going to be fine and representative of the physical reality.

Load application may then cause singularities, in particular if we are considering **point load forces** (i.e. force applied to a single node). The following image clearly shows the influence of the load type to the simulation results in terms of singularities.

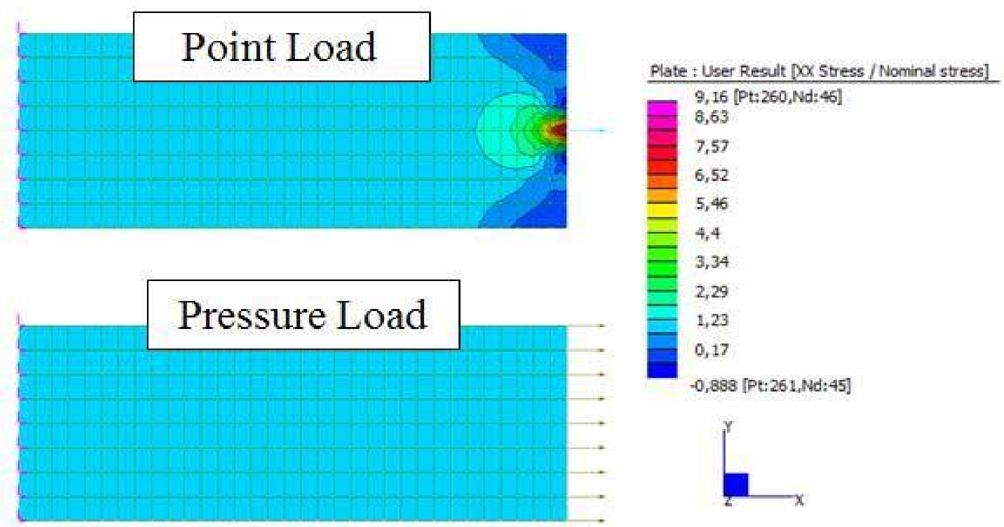

Figure 3-29 The influence of Point load in making singularities

When a load is applied to a simple plate, it is possible to define a certain distance 'b' where local effects are dominant. Out of this zone, according to Saint-Venant's Principle, stresses are no more affected by the method in which the load is applied [15].

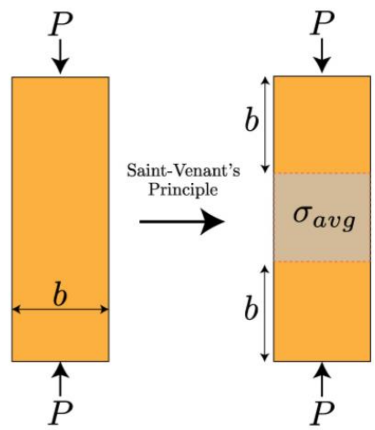

Figure 3-30 Defining a certain distance to consider load effect

Another typical situation where singularities occur are sharp **re-entrant corners**. These are points where the geometry shows an angle lower than 180°. In the example showed, we have a 90° angles. Once again, even if we note the stress singularity at the corner, it is possible to neglect it according to the above-mentioned principle. In a real geometry, since no corner is actually perfect, a small fillet radius is present. This means that in reality infinite stress obviously cannot occur. We generally see stress concentration instead [16].

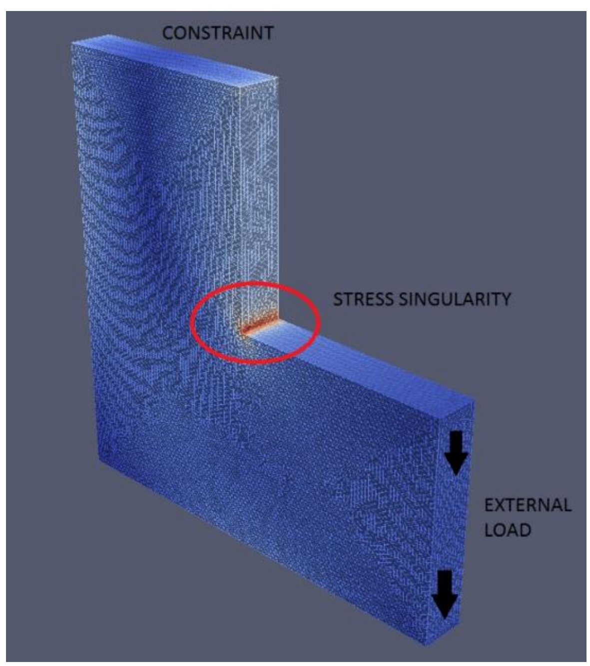

Figure 3-31 Simple 90° corner with sharp edge. Local effect in stress singularity

3.5.4 Stress concentration

Now it is the time to get into the details of a similar phenomenon: **stress concentration**. What now happens is something similar to a singularity point, but this time the *stress converge towards a finite value the more we refine our mesh*. This sort of behavior is due to the presence of a geometrical feature that somehow deflect the load pattern inside of our body [17]. For example a hole in a plate.

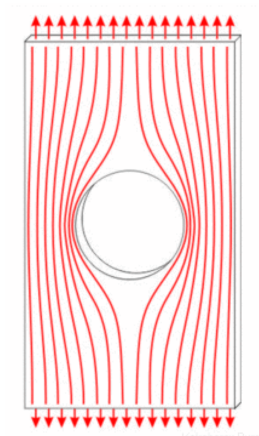

Figure 3-32 Example of a hole inside a plate. Stress concentration occur at the two side of the hole, where loads lines tend to gets closer and closer

In Figure 3-32, showing stress concentration around a small circular hole, we see that on the two sides of the hole stress field tend to become more intense. This is, obviously, due to the geometry we are analyzing and FEM analysis is able to capture this behavior (as long as the mesh is refined enough!). In general, for such type of plate, it is possible to define a concentration factor, ratio between the maximum stress and the average stress in the undisturbed plate, named **nominal stress**. In literature is possible to find out many relations to find out the stress factor as in [18] and [19].

In FEM (Finite Element Method), the user has the great responsibility of detecting singularities and distinguish between them and concentration points. Obviously, a mesh sensitivity study is mandatory to find out details about the case we are performing. In general it is possible to say that the main difference between the two behaviors is that singularities tends to have infinite stress as long as we refine the mesh, whilst concentrations tends to assume a finite value.

3.5.5 Nonconforming Mesh

A *nonconforming mesh* occurs when the shape functions in two connected elements do not match. The most common case is when an assembly is connected using identity pairs and continuity conditions. To exemplify this, we can study a straight bar with an intentionally nonmatching mesh. With a simple load case, such as uniaxial tension, it is possible to study the stress disturbances caused by the transition [20].

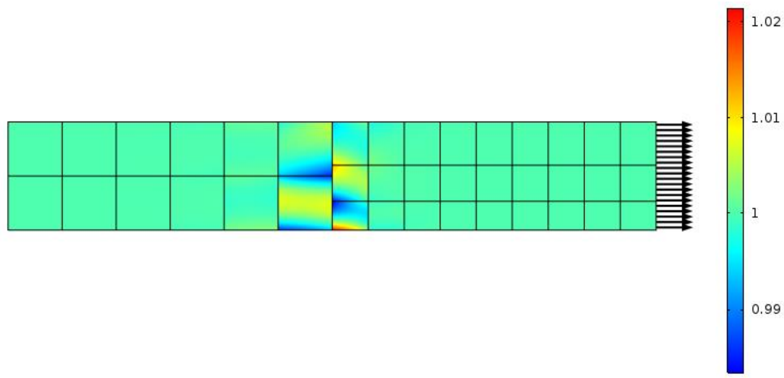

Figure 3-33 Axial stress at a nonconforming mesh transition. Second-order elements are used.

The forces transmitted by the nodes at the two sides do not match the assumption of constant stress. Again, this can be seen as a local load redistribution over an area that is the element size. Using the reasoning of Saint-Venant, the disturbance should fade away at an "element-sized" distance from the transition. Let's investigate what happens if the mesh is refined in the axial direction.

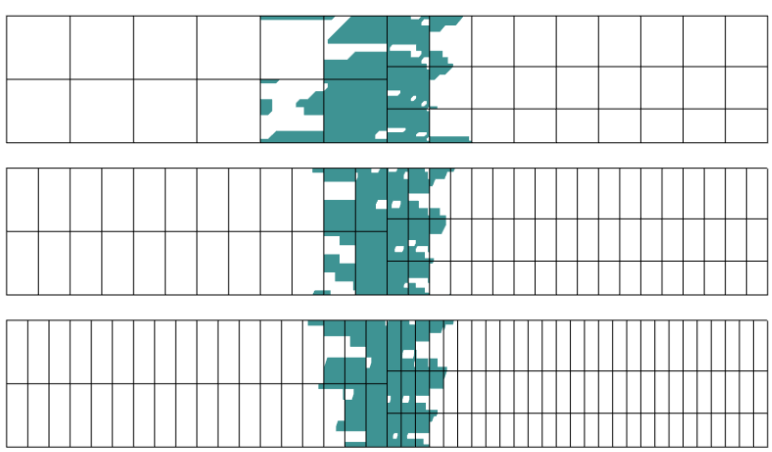

Figure 3-34 Region with more than 0.1% error in stress. Three different discretizations are used in the axial direction.

It turns out that the region of disturbance is not affected much by the discretization in the direction perpendicular to the transition boundary. This is exactly what Saint-Venant's principle tells us.

3.5.6 What is the difference between the stress concentration factor and stress intensity factor?

The stress concentration factor is a number that raises stress locally due to factors such as holes and changes in cross section. In the latter case, the sharper the radius at the cross-section changes, the higher the stress concentration. Typically, these factors range from 1.0 to 3.0 and sometimes more. The stress intensity factor is a bit different; it is an inherent property of the material that is tested and defined for cracks or flaws. For cracks and flaws, the radius is very small, approaching zero for sharp corners, and stress concentration factors become very high, approaching infinity [21]. In this case, we use the measured stress intensity factor and equations of fracture mechanics to calculate allowable stresses. It is often used for fatigue calculations for metals and for strength determination for brittle materials like glasses and ceramics.

3.5.7 Stress concentration factor

A stress concentration factor (Kt) is a dimensionless factor that is used to quantify how concentrated the stress is in a mechanical part. It is defined as the ratio of the highest stress in the part compared to a reference stress [22].

$$\sigma_{\max} = K_t \sigma_{ave}$$

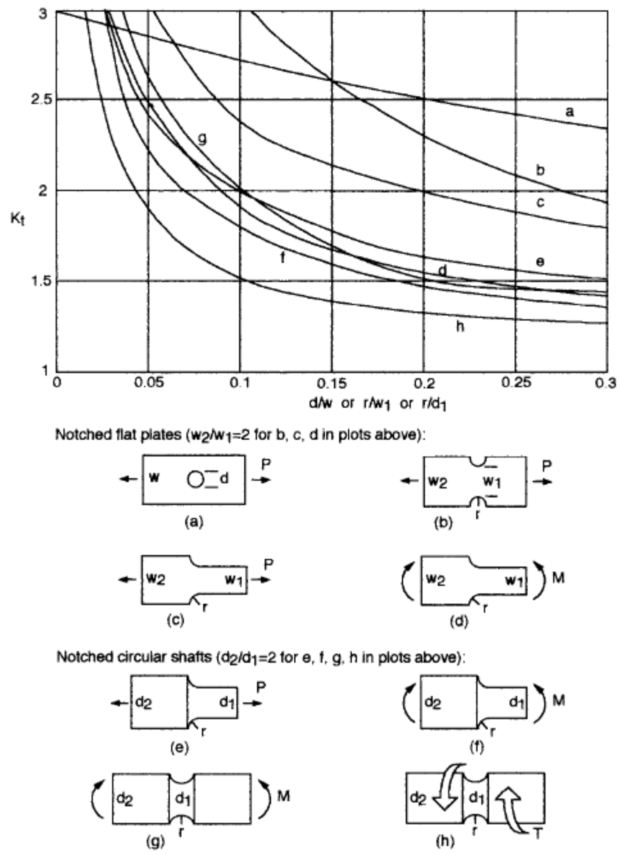

Figure 3-35 The way stress concentration factor calculated

There are experimental methods for measuring stress concentration factors including photo-elastic stress analysis, thermos-elastic stress analysis, brittle coatings or strain gauges.

During the design phase, there are multiple approaches to estimating stress concentration factors. Several catalogs of stress concentration factors have been published. Perhaps most famous is *Stress Concentration Design Factors* by Peterson, first published in 1953. Finite element methods are commonly used in design today [23].

3.5.8 Calculation of safety factor 2

Regarding all mentioned above, we want to report maximum stress for each part and then calculate FS. This time in each part, when the numerical simulation displays the maximum stress, first, it is necessary to check its' region and the potential of stress concentration. If there is stress concentration, we should recalculate the stress with the method discussed in the above section, and then if the stress were still the maximum one in that part, it would be the amount used to calculate the FS. Consequently, the amount of FS for each part would be in the following table:

Table 3-7 FS values in the pole components (considering stress concentration factor)

Part	Max σ_{VM} [MPa]	YS [MPa]	FS	FS improvement
Pole ZP2-10 (upper part)	195	420	2.15	53%
Pole ZP2-10 (lower part)	270	420	1.55	55%
Hat	176.8	420	2.37	-
Bracket	191.7	420	2.19	-

After considering the Stress concentration factor method, the maximum stress in the ZP-2 part changed dramatically which influence the value calculated for the FS. This improvement in FS is only the result of correction in stress calculation. Here in ZP-2, numerical simulation, because of stress concentration, reported stress more than real value and this method helps to compensate this error, have the lower values of stress and higher FS without the necessity of improving the design.

3.5.9 Conclusion

In this thesis, we wanted to show reliable ways to evaluate the strength of poles. All of these analyses are done to decrease the need for crash tests and to save money. In this way, producers pay for the expensive crash test when they are sure that the structure will pass the test and is safe. As it was discussed in detail, when we want to evaluate the strength of a newly designed structure the following steps should be done to have a reliable answer on the basis of EN 12767:

1- Consider the pole cross-section,

2- If the cross-section is continuously Regular polygons:

2-1 Yes, Simple geometry:

There is a simple method to analyze the strength of poles, which is easy to implement, fast, and an inexpensive method to get the result. In this kind of poles, we made an excel file to evaluate the pole easily which only needed to import the geometry features of the pole and then get the result so fast. Simple pole in this part means a pole with Circular, Triangular, Diamond, Hexagonal, Octagonal, and Rectangular cross-section with uniform cross-section from bottom to the top or at least near to this approximation.

2-2 No, Complex geometry:

The only choice is using numerical simulation and obviously, it takes more time and cost in comparison with the previous way. By performing the numerical simulation we get this result that related to each specific geometry it is possible to have diverse places as the critical regions. The simulation indicates these regions with high accuracy and the design improvement would be easier. In addition, it costs less in comparison with the situation we are not informed of the exact failure regions which we did not have in the excel file.

It is noticeable that always getting a correct answer from numerical simulation has some difficulties. Numerical simulation is really less expensive than a crash test and it can be a good alternative to a crash test when our results are really similar to what happens in the test. There are some common challenges in this way of solution such as stress concentration especially in dealing with complex geometries of poles. There are predefined ways to tackle stress concentration problems helping to have a reliable solution in this kind of trouble. We collected these sources of stress concentrations and also the way it is possible to shift from just numerically increased stress to the real values. We could see that when there is a rocket in stress values only for one element and not in a region of elements, it is exactly the place we have the stress concentration. After recognition of these places in the result, with getting advantage of the stress concentration factor we would practically be able to reach correct values of stress. After that we should calculate the safety factor and consequently, we do not have the influence of numerical errors in our calculations.

In the following flowchart the above steps displayed graphically:

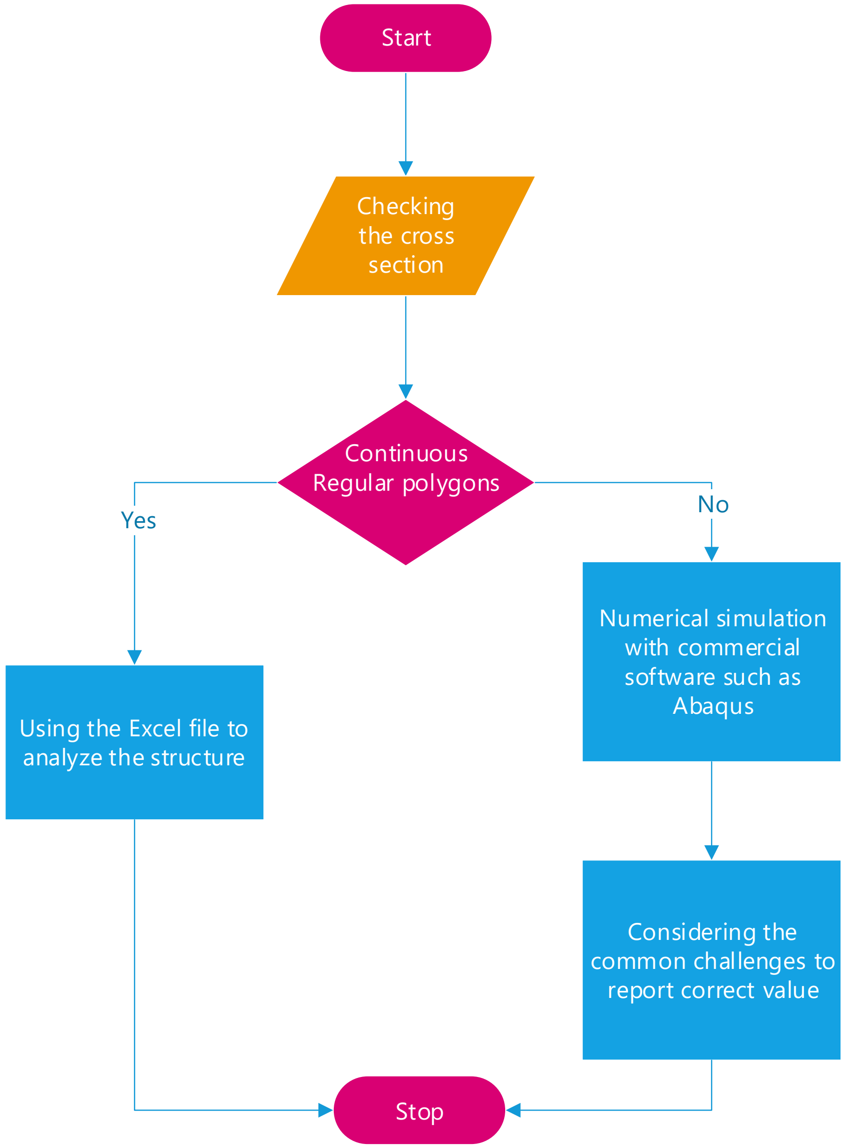

Figure 3-36 The flowchart showing the process to have a valid analysis

3.5.10 Recommendation

On the basis of the numerical simulation done in this thesis, it is obvious that EN standards define the loads and conditions to analyze the structure but at present time there is not any obligation to force manufactures to implement numerical simulation for their complex products and in this situation, the judgment performed by simple calculation (like the Excel file) has the potential to be far from correct values of stress. Producers prefer to pay less when they want to get a certificate and for sure an estimation assumed complex geometry like a simple one costs less. This is the point in some case may provide the possibility of mistakes in judgment. Therefore, it is needed to introduce finite element simulations as a proven way of analysis to be mandatory instead of simple analysis like Excel sheet files when dealing with complex geometries.

4 Appendix 1

Shape	surface 1	surface 2	surface 3	surface 4
Circular	0.79	0.00	0.00	0.00
Diamond	0.50	0.00	0.00	0.00
Hexagonal	0.87	0.00	0.00	0.00
None	0	0	0	0
Octogonal	0.83	0.00	0.00	0.00
Rectangular	1.00	0.00	0.00	0.00
Triangular	0.43	0.00	0.00	0.00
Eccentricity	0.5285	0	0	0

Circular signs:	S = 0,25 π W² = 0,785 W²
Diamondshaped signs:	S = 0,5 W²
Hexagonal signs :	S = W² cos 30° = 0,866 W²
Octogonal signs :	S = 2 W² tg 22,5° = 0,828 W²
Rectangular signs :	S = W x H
Triangular signs :	S = 0,5 B² cos 30° = 0,433 B²

* Note: This table is filled automatically as a function of the signs input geometry

Signs data

Sign number (maximum 4)	Sign 1	Sign 2	Sign 3	Sign 4
Sign Shape	Circular	None	None	None
Sign Width W [m]	1	0	0	0
Sign Height H [m]	1	0	0	0
Height above ground A [m]	1	0	0	0
Sign surface eccentricity SE [m] [+ or -]	0.0285	0	0	0
Sign surface [m²]	0.785	0	0	0
Height of the CoG [m]	1.5	0	0	0

Supports data

Number of Supports	1	
Material	Steel S	235
Cross section	CHS	
Outer Diameter, Dp [mm]	57	
Wall Thickness, T [mm]	5	
Total Length of Support, L [m]	2.00	
Moment of Inertia, I [mm⁴]	278636	278494
Modulus of Elasticity, E [N/mm²]	210000	
Shear modulus, G [N/mm²]	81000	
Support Stiffness, EI [KNm²]	58.51	
Torsional constant, I_T [mm⁴]	557271	
Resistance modulus, W [mm3]	9776.7	
Shear area of the CS, Av [mm²]	520.0	
Torsion area of the CS, Am [mm²]	2123.7	

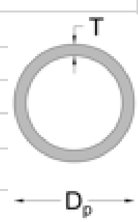

CHS

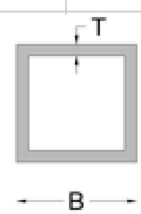

SHS

Cross section	
Circular Hollow Section	CHS
Squared Hollow Section	SHS

	Material	f_y [MPa]	f_u [MPa]	β_w
Steel	S 235	235	360	0.8
	S 275	275	430	0.85
	S 355	355	510	0.9
	S 420	420	520	1
	S 450	450	550	1
	S 460	460	540	1
Aluminium	Al	240		

Hollow Rectangle Thin Walled

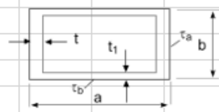

$$J' = \frac{2.t.t_1.(a-t)^2.(b-t_1)^2}{a.t + bt_1 - t^2 - t_1^2}$$

$$\tau_{average}\ \tau_a = \frac{T}{2.t.(a-t).(b-t_1)}$$

$$\tau_{average}\ \tau_b = \frac{T}{2.t_1.(a-t).(b-t_1)}$$

Higher stresses at internal corners unless large fillet radii used

Shear area, Av according to EN 1993-1-1:2005

f) rolled rectangular hollow sections of uniform thickness:	
load parallel to depth	Ah/(b+h)
load parallel to width	Ab/(b+h)
g) circular hollow sections and tubes of uniform thickness	2A/π

Loading conditions

Wind load (per class) [kN/m²]	WL3	0.80
Point load (per class) [kN]	PL2	0.30

Temporary deflection criteria

Maximum temporary deflection - Bending [mm/m]	TDB3	10
Maximum temporary deflection - Torsion [°/m]	TDT4	0.29

Safety factors

Safety class	PAF1
Loads Partial Safety Factor, γ_F	1.35
Materials Partial Safety Factor, γ_m	1.05
Shape Factor, C_f	1.2
Wind Pressure Coefficient, c_w	0.56

2. Temporary deflection checks

*Note: The wind load is multiplied by c_w and no partial action and material factors are applied.

Loads (wind load only)

Characteristic Wind Pressure [kN/m²]	0.80
Design Wind Pressure [kN/m²]	0.54

Bending

	Sign 1	Sign 2	Sign 3	Sign 4	
Design Wind Load [kN]	0.42	0	0	0	
Deflection for each sign level - Bending [mm]	12.18	0	0	0	
Total deflection at the top of the support [mm]	12.177				
Temporary deflection - Bending (relative) [mm/m]	6.09				
Check: Temporary deflection - Bending	61%				PASS

Torsion

	Sign 1	Sign 2	Sign 3	Sign 4	
Rotation for each sign level [rad]	3.4E-13	0	0	0	
Total rotation - upper end of the support - torsion [rad]	3.39432E-13				
Temporary rotation - Torsion (relative) [°/m]	9.724E-12				
Check: Temporary deflection - Torsion	0%				PASS

3. Permanent deflection checks

*Note: The wind load is multiplied by C_f and partial action and material factors are applied.

Loads

Characteristic Wind Pressure [kN/m²]	0.80
Point Load [kN]	0.30
Design Wind Pressure [kN/m²]	1.296
Design point Load [kN]	0.405

Wind Load: Base Bending Moment

	Sign 1	Sign 2	Sign 3	Sign 4	
Design Wind Load [kN]	1.02	0	0	0	
Base Bending Moment due to each sign [kNm]	1.53	0	0	0	
Total Base Bending Moment, M_{Ed} [kNm]	1.527				
Yield limit stress, f_y [N/mm^2]	235				
Bending capacity, M_{Rd} [kNm]	2.19				
Normal stresses - Bending, σ [N/mm^2]	156.17				< 235
Check: Bending resistance	70%				PASS

Wind Load: Torsion

	Sign 1	Sign 2	Sign 3	Sign 4	
Design Wind Load [kN]	1.018	0	0	0	
Torsion at the level of each sign [kNm]	0.02901	0	0	0	
Total Torsion at the base of the suport [kNm]	0.029009467				
Shear yield limit stress, τ_y [N/mm2]	135.7				
Torsion capacity, T_{Rd} [kNm]	2.53				
Shear stresses - Torsion, τ_t [N/mm^2]	1.37				< 135.7
Check: Torsion resistance	1%				PASS

Wind Load: Shear

	Sign 1	Sign 2	Sign 3	Sign 4	
Design Wind Load [kN]	1.018	0	0	0	
Design Shear Force, V_{Ed} [kN]	1.018				
Shear Capacity of the suport, V_{Rd} [kN]	70.56				
Shear stresses - Shear, τ [N/mm^2]	1.96				< 135.7
Check: Shear resistance	2%				PASS

Wind Load: Overall check

Equivalent (von Mises) stresses - Bending, σ_e [N/mm^2]	156.3		
Elastic stress verification	0.40	<= 1	PASS

Horizontal Point Load (on the upper sign): Base Bending Moment

Upper Sign	Circular	
Number of signs	1	
Design Point Load [kN]	0.405	
Height of the CoG [m]	1.5	
Base Bending Moment, M_{Ed} [kNm]	0.608	
Yield limit stress, f_y [N/mm^2]	235	
Bending capacity, M_{Rd} [kNm]	2.19	
Normal stresses - Bending, σ [N/mm^2]	62.14	< 235
Check: Bending resistance	28%	PASS

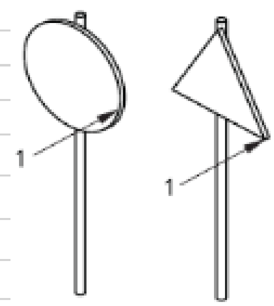

Horizontal Point Load (on the upper sign): Torsion

Design Point Load [kN]	0.405	
Load application eccentricity (LE) [m]	0.5285	
Total Torsion at the base of the suport [kNm]	0.21	
Shear yield limit stress, τ_y [N/mm2]	135.7	
Torsion capacity, T_{Rd} [kNm]	2.53	
Shear stresses - Torsion, τ_t [N/mm^2]	10.08	< 135.7
Check: Torsion resistance	2%	PASS

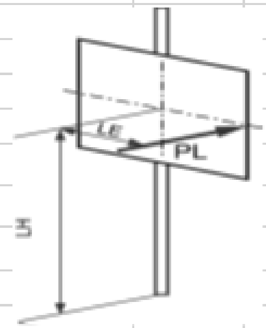

Horizontal Point Load (on the upper sign): Shear

Design Point Load [kN]	0.405	
Shear Capacity of the suport, V_{Rd} [kN]	70.56	
Shear stresses - Shear, τ [N/mm^2]	0.78	< 135.7
Check: Shear resistance	0%	PASS

Point Load: Overall check

Elastic stress verification	0.08	PASS
	<= 1	

Vertical Point Load (on the widest sign): Base Bending Moment

Upper Sign	Circular	
Number of signs	1	
Design Point Load [kN]	0.405	
Load application eccentricity (LE) [m]	0.5285	
Base Bending Moment, M_{Ed} [kNm]	0.214	
Yield limit stress, f_y [N/mm^2]	235	
Bending capacity, M_{Rd} [kNm]	2.19	
Normal stresses - Bending, σ [N/mm^2]	21.89	< 235
Check: Bending resistance	7%	PASS

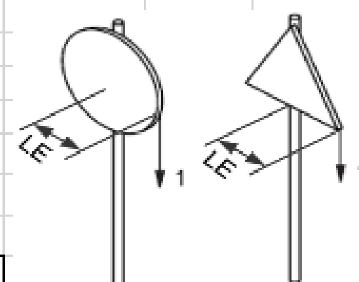

5 Appendix 2

5.1.1 Assembly and Step module

In Assembly module, we just call and create the instances from the part module and consider 'Static, General' in procedure type. Because our problem is a static analysis [24].

5.1.2 Interaction module

If start from bottom to the top of the pole, first we have the overlap region between ZP2-10 upper and lower part which should be defined. There are two rows of rivets in this region to make this connection.

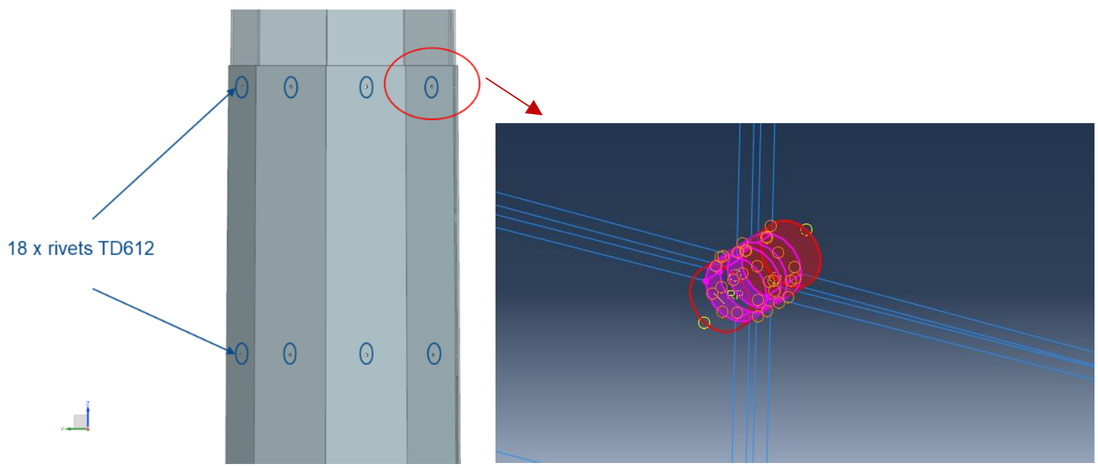

Figure 5-1 Details of interactions considered between ZP2-10 upper and lower part

With using 'Tie' constraint, the connection created. The rivet is the master surface tied in connected surfaces with upper and lower ZP2.

Next interaction defined for ZP2 (both parts). The structure of ZP2 is made of a plate that has bended and as you see in the bellow picture, there are some Rivets in the region the plate has overlap with tie interaction (This is the same interaction for all rivets in both upper and lower part of ZP2)

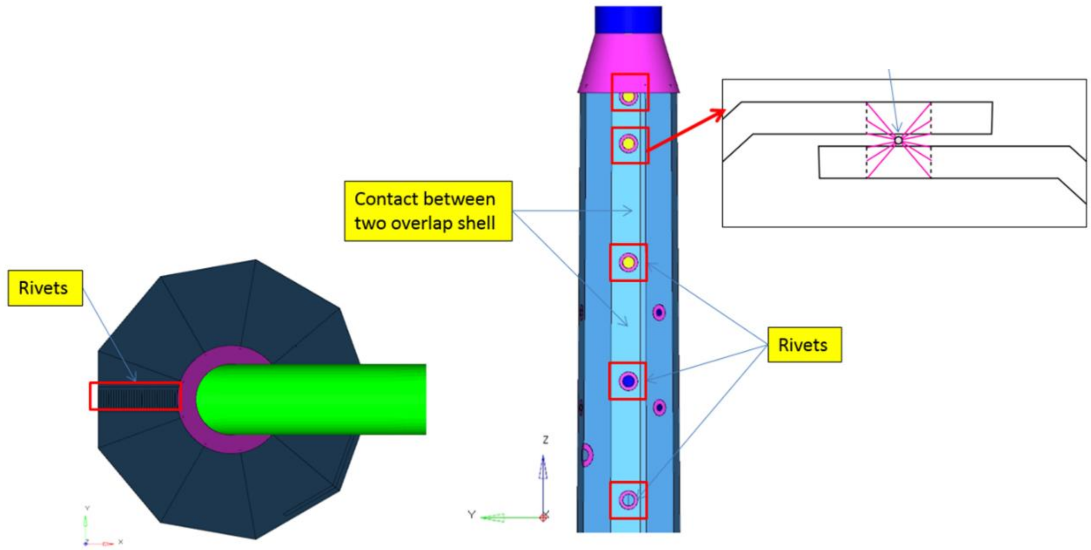

Figure 5-2 Tie interaction defined in rivets where two overlap contact

There is a bolt (M10) to connect ZP2 (Upper part) to the bracket. It is a bolt, which pass through the whole width. There is tie connections between bolt (as the master) and contact cross-section of bracket and ZP2 (as the slaves).

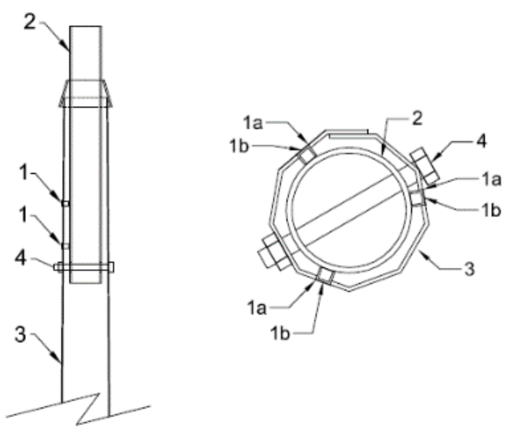

N°	Description	#
1a 1b	rivet nut M6 positioning bolt M6	6 6
2	bracket Ø60,3	1
3	column	1
4	bolt M10	1

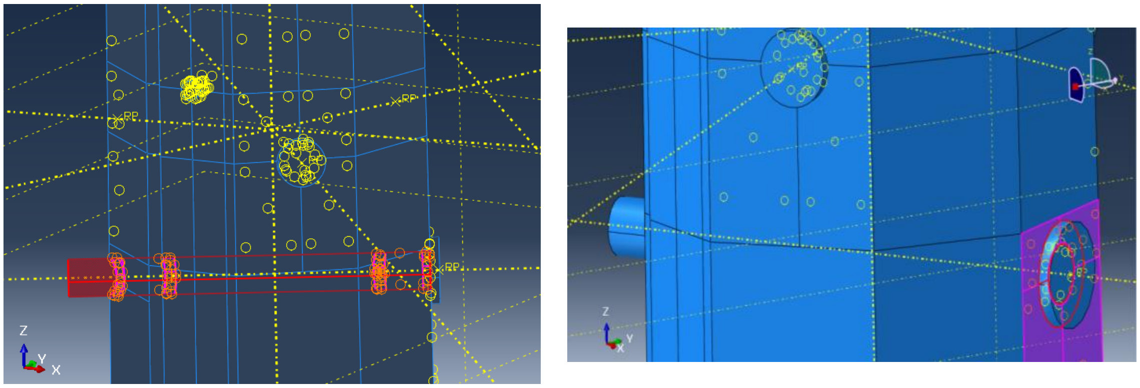

Figure 5-3 Details of the tie interaction considered for the central bolt

To maintain the bracket, There are six M6 rivets to make connection between ZP2 (upper part) and bracket. Again, tie connection defined to connect head bolt to the ZP2 and bottom of bolt to the bracket.

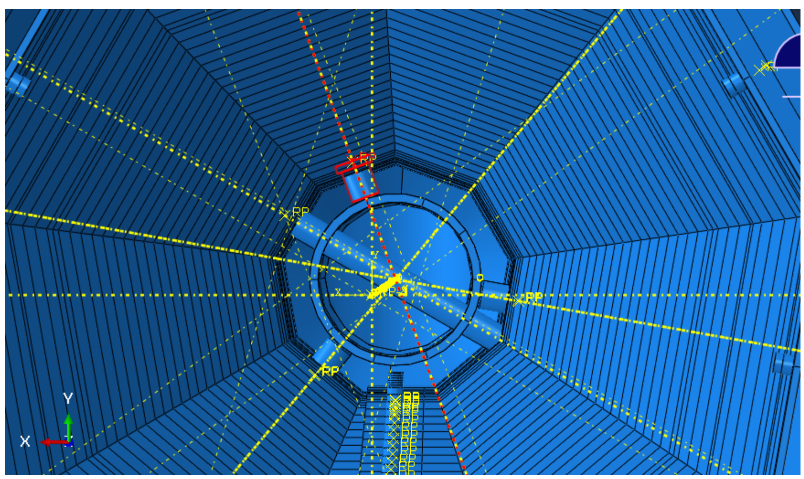

Figure 5-4 Tie interaction defined for rivets between bracket and ZP2 (upper part)

At the end of ZP2 (upper part), there is a hat which is welded to bracket, to define this interaction in Abaqus, first there is a tie contact between hat and bracket and secondly, Surface to Surface interaction between hat and ZP2.

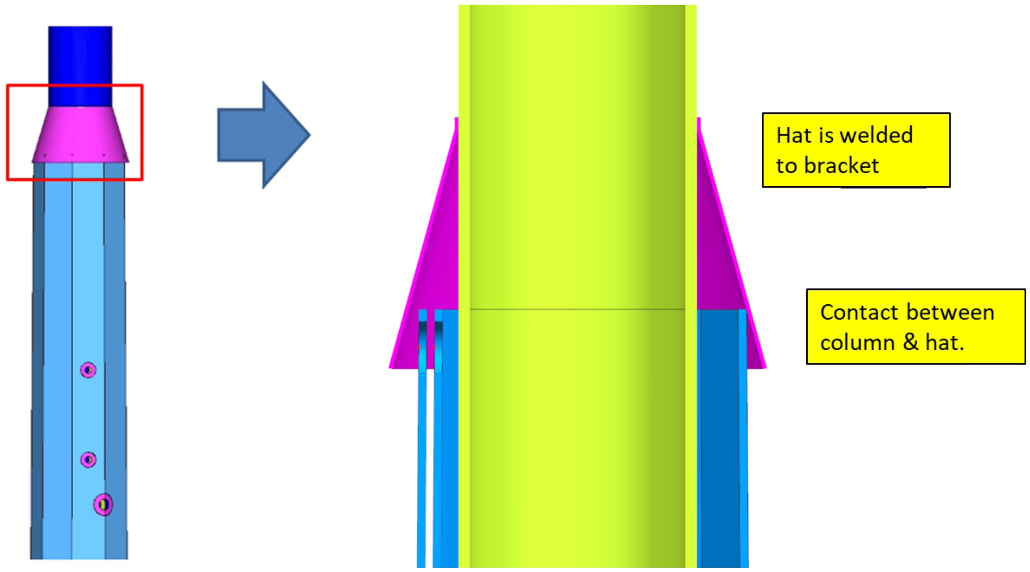

Figure 5-5 two *interaction* in upper and lower part of hat

5.1.3 Load module

Next step is defining Loads and boundary conditions. From the top, there is 20Kg as a weight because of the lamp at the top pf the bracket. Structural load with considering the material (defined in property module) and the gravity is taken into account from top to bottom.

The whole structure exists inside a hole and surrounded by concrete. Consequently, from the bottom of ZP2 until 900mm height was fixed (all degrees of freedom closed for this region).

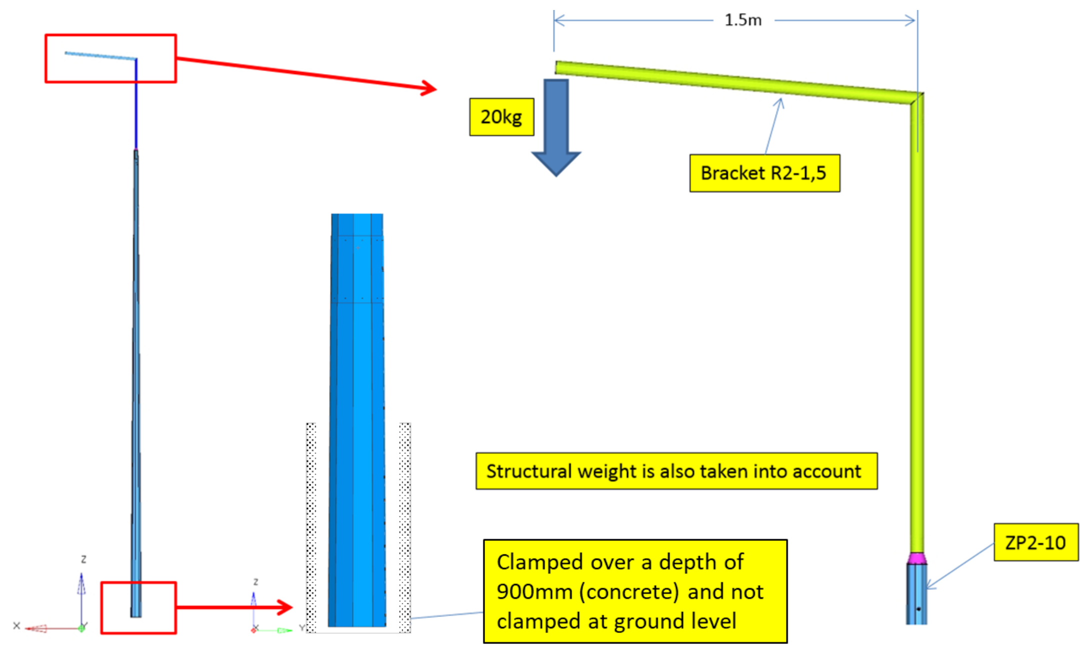

Figure 5-6 The completely fixed region of ZP2

Finally, we should define wind load as the input load for the structure. Wind forces are given by SAFETY-PRODUCT in a table of the file called « 12ZP2-10R2-1.5 voor NE paal.xls »

								Total Forces affected by the γ_f factor					
Column diameter or Distance across flats	D							Force exerted by wind				Dead load	
Projection of the considered part of the bracket	P							about x-x axis		about y-y axis		about y-y axis	
Thickness of metal	t												
	Shape	z_{mean} (m)	Δz (m)	D_{mean} (m)	P_{mean} (m)	ΔP (m)	F per m² (N/m²)	A (m²)	$F^*\gamma_f$ (N)	A (m²)	$F^*\gamma_f$ (N)	V (dm³)	$F^*\gamma_f$ (N)
Column Shaft	2	0.00		0.22	0.00	0.00							
1	2	0.30	0.60	0.21	0.00	0.00	**962**	0.13	145	0.13	145	0.822	76
2	2	0.80	0.40	0.20	0.00	0.00	**966**	0.08	94	0.08	94	0.533	50
3	2	1.25	0.50	0.20	0.00	0.00	**971**	0.10	114	0.10	114	0.644	60
4	2	1.75	0.50	0.19	0.00	0.00	**976**	0.09	111	0.09	111	0.621	58
5	2	2.25	0.50	0.18	0.00	0.00	**981**	0.09	107	0.09	107	0.599	56
6	2	2.75	0.50	0.18	0.00	0.00	**986**	0.09	104	0.09	104	0.576	54
7	2	3.25	0.50	0.17	0.00	0.00	**991**	0.08	100	0.08	100	0.553	51
8	2	3.75	0.50	0.16	0.00	0.00	**996**	0.08	97	0.08	97	0.531	49
9	2	4.25	0.50	0.16	0.00	0.00	**1019**	0.08	95	0.08	95	0.508	47
10	2	4.75	0.50	0.15	0.00	0.00	**1058**	0.07	94	0.07	94	0.485	45
11	2	5.25	0.50	0.14	0.00	0.00	**1094**	0.07	93	0.07	93	0.462	43
12	2	5.75	0.50	0.13	0.00	0.00	**1128**	0.07	91	0.07	91	0.440	41
13	2	6.25	0.50	0.13	0.00	0.00	**1161**	0.06	89	0.06	89	0.417	39
14	2	6.75	0.50	0.12	0.00	0.00	**1192**	0.06	87	0.06	87	0.394	37
15	2	7.25	0.50	0.11	0.00	0.00	**1222**	0.06	84	0.06	84	0.372	35
16	2	7.75	0.50	0.11	0.00	0.00	**1251**	0.05	80	0.05	80	0.349	32
17	2	8.25	0.50	0.10	0.00	0.00	**1278**	0.05	77	0.05	77	0.326	30
18	2	8.75	0.50	0.09	0.00	0.00	**1306**	0.05	73	0.05	73	0.303	28
19	2	9.25	0.50	0.09	0.00	0.00	**1332**	0.04	69	0.04	69	0.281	26
20	2	9.75	0.50	0.08	0.00	0.00	**1358**	0.04	65	0.04	65	0.258	24
Sum of wind forces *(or dead load)* on Column Post									1870		1870		*881*
1st Bracket	1	10.00		0.06	0.00	0.00							
1	1	10.50	1.00	0.06	0.00	0.00	**1280**	0.06	93	0.06	93	0.523	49
2	1	11.50	1.00	0.06	0.00	0.00	**1311**	0.06	95	0.06	95	0.523	49
3	1	12.00	0.00	0.06	0.00	0.00	**1326**	0.00	0	0.00	0	0.000	0
4	1	12.00	0.00	0.06	0.00	0.00	**1326**	0.00	0	0.00	0	0.000	0
5	1	12.00	0.00	0.06	0.00	0.00	**1326**	0.00	0	0.00	0	0.000	0
6	1	12.00	0.00	0.06	0.00	0.00	**1326**	0.00	0	0.00	0	0.000	0
7	1	12.00	0.00	0.06	0.00	0.00	**1326**	0.00	0	0.00	0	0.000	0
8	1	12.00	0.00	0.06	0.00	0.00	**1326**	0.00	0	0.00	0	0.000	0
9	1	12.03	0.07	0.06	0.37	0.75	**1327**	0.05	72	0.00	6	0.392	36
10	1	12.10	0.07	0.06	1.12	0.75	**1329**	0.05	72	0.00	6	0.392	36
Sum of wind forces *(or dead load)* on 1st Bracket									332		200		*170*
1st Lantern	1	12.13	0.00	1.00	1.49	0.00							
1	1	12.63	1.00	1.00	1.49	0.00	**224**	1.00	269	*1.00*	269		235
Sum of wind forces *(or dead load)* on 1st Lantern									269		269		235

Figure 5-7 wind load as the input load for the structure

In accordance to this input data, loads considered in each point and in X-direction.

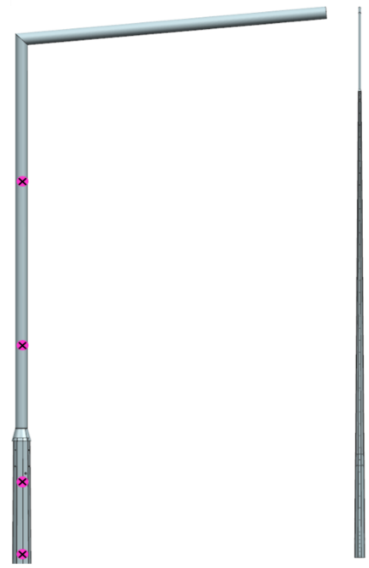

Figure 5-8 Different wind load applied in function of the height (Zmean=0 at ground level).

5.1.4 Mesh module

Mesh is created for each part separately and to have better quality of mesh, so many partition created.

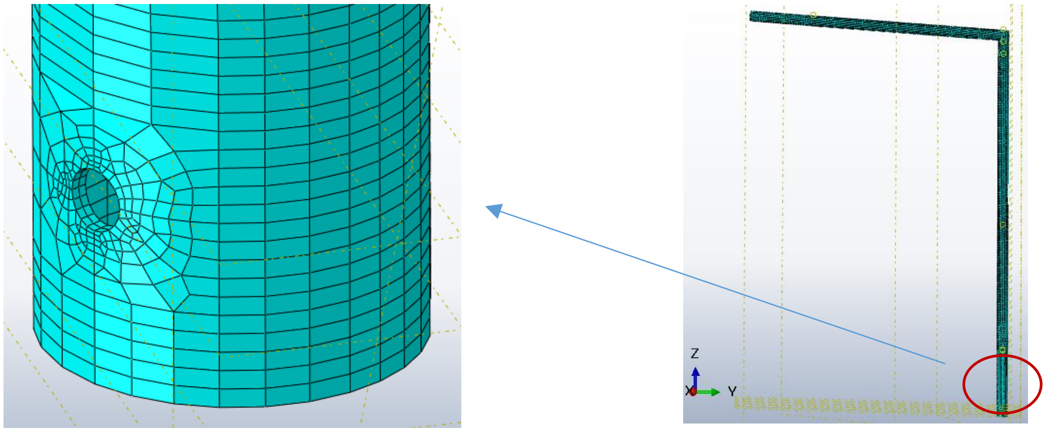

Bracket

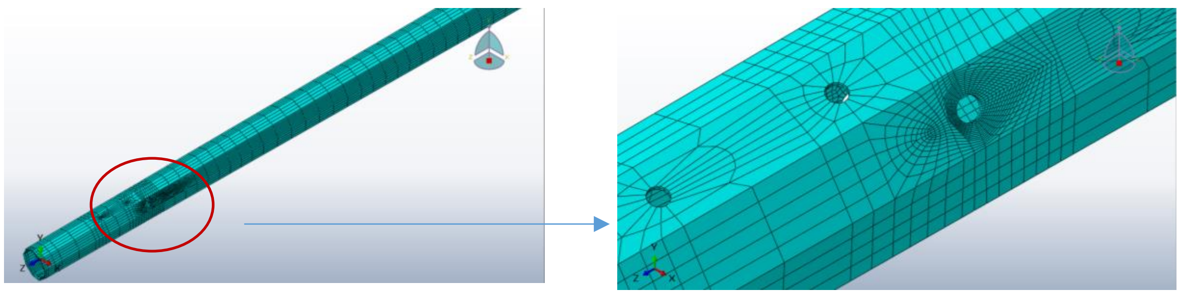

ZP2 upper part

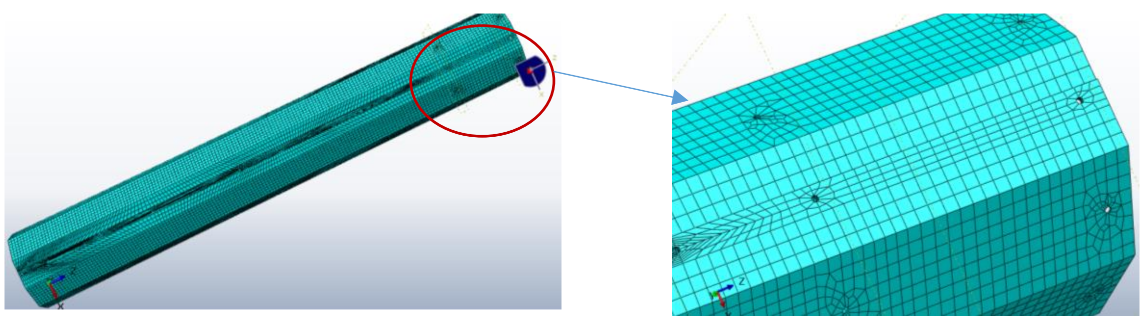

ZP2 lower part

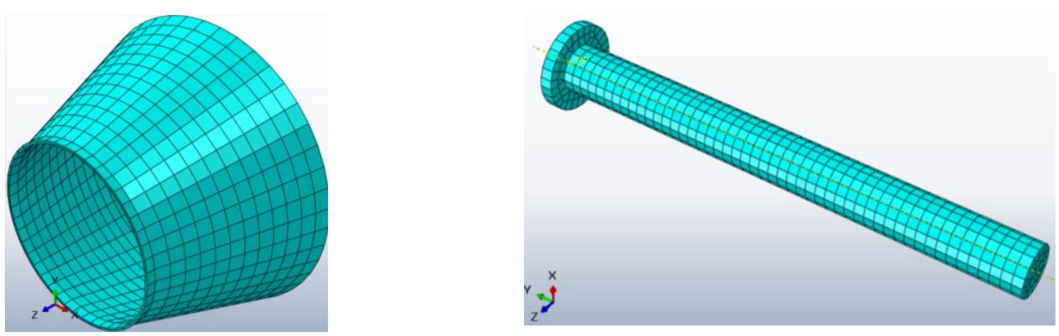

Bracket Bolt

Figure 5-9 Different views of genration Mesh in the pole components

6 References:

[1] Simpson, D. "EN 12767-a new tool in accident reduction." Traffic engineering & control 41.7.(2000)
[2] Beer, F. P., Johnston, E. R., DeWolf, J. T., & Mazurek, D. F. (2014). Mechanics of Materials. 7th Editio.
[3] Reiner, Johannes, and Reza Vaziri. "8.4 Structural analysis of composites with finite element codes: An overview of commonly used computational methods." (2018): 61-84.
[4] Bucalem, M. L., and Klaus-Jurgen Bathe. "Finite element analysis of shell structures." Archives of Computational Methods in Engineering 4.1 (1997): 3-61.
[5] Van der Ploeg, A., Eugen Foppe Franz Botta, and Friederik Wilhelm Wubs. "Grid-independent convergence based on preconditioning techniques." Multigrid Methods IV. Birkhäuser, Basel, 1994. 333-344..
[6] Schnack, Eckart. "An optimization procedure for stress concentrations by the finite element technique." International Journal for Numerical Methods in Engineering 14.1 (1979): 115-124
[7] Budzynski, Marcin, et al. "The role of numerical tests in assessing road restraint system functionality." European Transport Research Review 12 (2020): 1-11.
[8] Barth, Tim. "A brief overview of uncertainty quantification and error estimation in numerical simulation." NASA Ames Research Center, NASA Report.(2011)
[9] Budzyński, Marcin, et al. "Road restraint systems as a basis for roadside safety improvement." IOP Conference Series: Materials Science and Engineering. Vol. 471. No. 6. IOP Publishing, 2019.
[10] De Weck, Olivier, and Il Yong Kim. "Finite element method." Massachusetts Institute of Technology (2004): 1-26.
[11] Saneie, Hamid, et al. "Challenges of finite element analysis of resolvers." IEEE Transactions on Energy Conversion 34.2 (2018): 973-983.
[12] Toupin, Richard A. "Saint-Venant's principle." Archive for Rational Mechanics and Analysis 18.2 (1965): 83-96.
[13] Paushkin, Alexander, and Sergey Saiyan. "Numerical study of the applicability of the Saint-Venant principle." MATEC Web of Conferences. Vol. 117. EDP Sciences, 2017.
[14] Balijepalli, R. G., et al. "Numerical simulation of the edge stress singularity and the adhesion strength for compliant mushroom fibrils adhered to rigid substrates." International Journal of Solids and Structures 85 (2016): 160-171.
[15] Saint-Venant's Principle, Wikipedia, available at: http://es.wikipedia.org/wiki/Principio_de_Saint-Venant
[16] Carpinteri, Alberto. "Stress-singularity and generalized fracture toughness at the vertex of re-entrant corners." Engineering Fracture Mechanics 26.1 (1987): 143-155.
[17] Stowell, Elbridge Z. Stress and strain concentration at a circular hole in an infinite plate. Washington, DC: National Advisory Committee for Aeronautics, 1950.
[18] Young, W., Budynas, R., (2001), Roark's Formulas for Stress and Strain, Chapter 17 – Stress Concentrations, McGraw-Hill.
[19] Pilkey, D., Pilkey, W., (2008), Peterson's Stress Concentration Factors, Wiley; 3 edition.

[20] Kumar, Ashok V., et al. "Finite element analysis using nonconforming mesh." Journal of computing and information science in engineering 8.3.(2008)
[21] Newman, J. C., and I. S. Raju. "Stress-intensity factor equations for cracks in three-dimensional finite bodies." Fracture Mechanics: Fourteenth Symposium—Volume I: Theory and Analysis. ASTM International, 1983.
[22] Ozkan, Murat Tolga, and Ihsan Toktas. "Determination of the stress concentration factor (Kt) in a rectangular plate with a hole under tensile stress using different methods." Materials Testing 58.10 (2016): 839-847.
[23] Pilkey, Walter D., Deborah F. Pilkey, and Zhuming Bi. Peterson's stress concentration factors. John Wiley & Sons, 2020.
[24] Manual, Abaqus Scripting User'S. "Abaqus 6.11." http://130.149 89.2080 (2012): v6.